

## 2. AUTOMOTIVE ALUMINUM R&D

### A. Active Flexible Binder Control System for Robust Stamping

*Project Leader: Tom Balun*

*Ford Motor Company*

*Vehicle Operations General Office, C290, 17000 Oakwood Blvd.*

*Dearborn, MI 48121*

*(313) 322-4951; fax: (313) 845-2647; e-mail: tbalun@ford.com*

*Project Administrator: Mahmoud Y. Demeri*

*FormSys Inc.*

*40180 Woodside Drive South*

*Northville, MI 48167*

*(734) 462-2742; fax: (734) 462-2742; e-mail: mdemeri@formsysinc.com*

*Technology Area Development Manager: Joseph Carpenter*

*(202) 586-1022; fax: (202) 586-1600; e-mail: joseph.carpenter@ee.doe.gov*

*Field Technical Manager: Philip S. Sklad*

*(865) 574-5069; fax: (865) 576-4963; e-mail: skladps@ornl.gov*

---

*Contractor: U.S. Automotive Materials Partnership*

*Contract No.: DE-FC05-95OR22910*

---

#### **Objective**

- Develop and demonstrate, on an industrial scale, an optimized closed-loop flexible binder control system that can be installed in presses to improve the quality, reduce the variability, and maintain the accuracy of stampings made from aluminum alloys and ultra-high-strength and stainless steels. The system will also reduce the cost of developing and setting production tools.

#### **Approach**

- Conduct open-loop control demonstration of flexible binder technology.
- Develop methodology and guidelines for designing and building flexible binders.
- Develop computer simulation and process optimization capabilities for flexible binders.
- Develop a closed-loop flexible binder control system with appropriate sensors.
- Demonstrate closed-loop control of the flexible binder system on an industrial part.
- Evaluate technical and economic feasibility of flexible binder technology.

#### **Accomplishments**

- Conducted tests in a mechanical press to confirm the hydraulic reconfiguration necessary to obtain satisfactory closed-loop control in the hydraulic actuators of the Erie Binder Control Unit.

- Showed that the nonlinear control algorithm that has been validated in simulations and experimental tests provides effective closed-loop pressure control for constant and ramp step pressure profiles on a reconfigured cylinder from the Erie Unit.
- Began building a new tooling and binder control system at the University of Stuttgart (IFU). The tooling is based on a die design that included many features of automotive stampings (Hishida Die). The binder control system has special valves and controls for use in a mechanical press.
- Evaluated two methods, adaptive simulation (AS) and optimization (OPT), to predict feasible/optimum variable blank holder force (BHF) profiles for conical cup and rectangular pan drawing. Predictions were successfully verified by experimental results.
- Used AS and OPT methods to predict the variable BHF profiles for conical cups, rectangular pans, a tapered non-axisymmetric pan (Hishida part), and an S-rail. Experiments have also been conducted to verify the predicted optimum blank holder force profiles.
- Verified that variable BHF profiles improved the formability of conical cup drawing by about 9% compared with constant BHF profiles. Showed the importance of using results from AS as an initial guess for OPT in reducing the number of iterative simulation runs and computation time.
- Transferred the DOE-owned Binder Control Erie Unit to the U.S. Automotive Materials Partnership for use in the project.

### Future Direction

- Retrofit the Erie Binder Control Unit with a digital dSPACE real-time controller system to achieve hydraulic pressure control on all 26 cylinders in a mechanical press environment. Use the unit to conduct trials on a General Motors (GM) liftgate to determine the benefits of using flexible binder control technology in sheet metal stamping.
- Set up and conduct trials on the new IFU flexible binder control system to determine the benefits of using flexible binder control systems in improving the part quality and consistency in automotive stampings.
- Conduct experiments to determine the critical sidewall wrinkle amplitude predicted by PAM-STAMP (i.e., amplitude of 1.21 mm). The critical sidewall wrinkle amplitude would greatly affect the prediction of variable BHF profiles in AS and OPT.
- Develop a method for determining initial guesses for BHF for use in predicting BHF profiles using AS or OPT. (The BHF profiles predicted by both AS and OPT depend on the initial guess for the BHF.)
- Evaluate the fatigue properties and determine stress concentrations and allowable stresses in flexible binders.

---

### Introduction

Significant weight saving can be achieved by replacing parts made from mild steel with those made from lightweight materials (aluminum and magnesium alloys) and high specific strength materials (ultra-high-strength and stainless steels). Such materials are less formable than mild steel, and parts made from them lack dimensional control

because of the significant amount of springback that they produce after forming.

Traditional stamping leaves no flexibility in the stamping process for using difficult-to-form materials and for responding to process variations (lubrication, material, die wear, blank placement) that can lead to stamping inconsistencies or even failure. It has been found that failure by wrinkling or tearing is

highly dependent on the magnitude and trajectory of the binder force. Recently, dynamic variation of the binder force during the forming stroke has been shown to affect formability, strain distribution, and springback. Optimal forming trajectories can be obtained under constant and variable binder force conditions, but there is no guarantee that process variables will remain constant during the stamping process. Specifying a binder force trajectory is not easy because the part shape changes during forming. Also, stresses in the part cannot be determined because the coefficient of friction is not a controllable quantity and it varies from location to location. Therefore, the forming process must be controlled, and a closed-loop system with an appropriate local control parameter (friction, draw-in) must be used to track a predetermined optimum control parameter trajectory.

Flexible binder control technology will be used in conjunction with innovative tool designs and closed-loop control to produce robust processes for stamping aluminum and high-strength-steel automotive panels. The focus of the project is on implementing binder and feedback process control in the stamping industry to increase the robustness of the forming process and improve the quality and consistency of stampings. This technology will use computer simulation and process optimization to predict optimum binder force trajectories that can be entered into programmable hydraulic cushions to control binder actions in mechanical and hydraulic presses.

### **Open-Loop Control Demonstration of Flexible Binder Control Technology**

A two-path approach has been adopted for this task. The first one is to retrofit the existing Erie Unit with the appropriate real-time control system to achieve hydraulic pressure control in all 26 cylinders in a mechanical press environment. The unit will then be used as planned in conjunction with the liftgate tooling. The second path is to

have IFU build a more robust and industrially oriented smaller unit.

### **Retrofit the Existing Erie Binder Control Unit**

A single hydraulic cylinder test was conducted on a full-scale mechanical press at TDM in Warren, MI. The cylinder represented the force actuation component of a flexible binder unit. The objectives were to validate the mathematical models developed to represent the dynamics of the system and to validate the proposed nonlinear control strategy described in previous reports. A special hydraulic unit was constructed for this purpose. Figure 1 shows the single cylinder test setup in a mechanical press.

The tests showed that the mathematical model represented the dynamics of the system with good accuracy, and the closed-loop control results showed tracking performance within 10% of the commanded value in the critical operating range.



**Figure 1.** Single-cylinder test setup.

Tests were also conducted to confirm the hydraulic reconfiguration necessary to obtain satisfactory closed-loop pressure control in the hydraulic actuators of the Erie unit. The tests were conducted in a mechanical press with a peak ram speed of about 620 in./min.

The primary hydraulic problem observed was pressure spikes in the cylinder caused by the rod-side flow (upper and lower lines in Figure 2). Cylinder hydraulics were reconfigured to divert the rod-side flow directly to the tank. The reconfiguration eliminated the problem, and the pressure dynamics of the reconfigured system were close to the dynamics predicted by the mathematical model of the system. The nonlinear control algorithm that had been validated in previous simulations and tests was shown to provide effective closed-loop pressure control for constant and ramp-step pressure profiles on the reconfigured cylinder from the Erie unit.

### Build a New Binder Control Unit

The new IFU unit will have only ten cylinders to accommodate a generic tool that captures the main features of industrial stampings. It will have state-of-the-art cylinders, valves, and controls and will accommodate three types of sensors for use in closed-loop control of the binder in a mechanical press environment. User interface with the system will be through a touch screen by which individual cylinder pressure may be selected. Figure 3 shows the IFU unit after the integration of a new valve block. The diagram gives the overall dimensions of the unit and shows the pyramidal pattern of the lower flexible binder and the lightweight structure of the upper binder.

Proportional valves are used to control pressure during the forming process. Initial pressure control tests on the valves showed good performance as indicated by a position control value of  $\pm 0.2$  mm and a pressure change speed of 2000 bar/s.

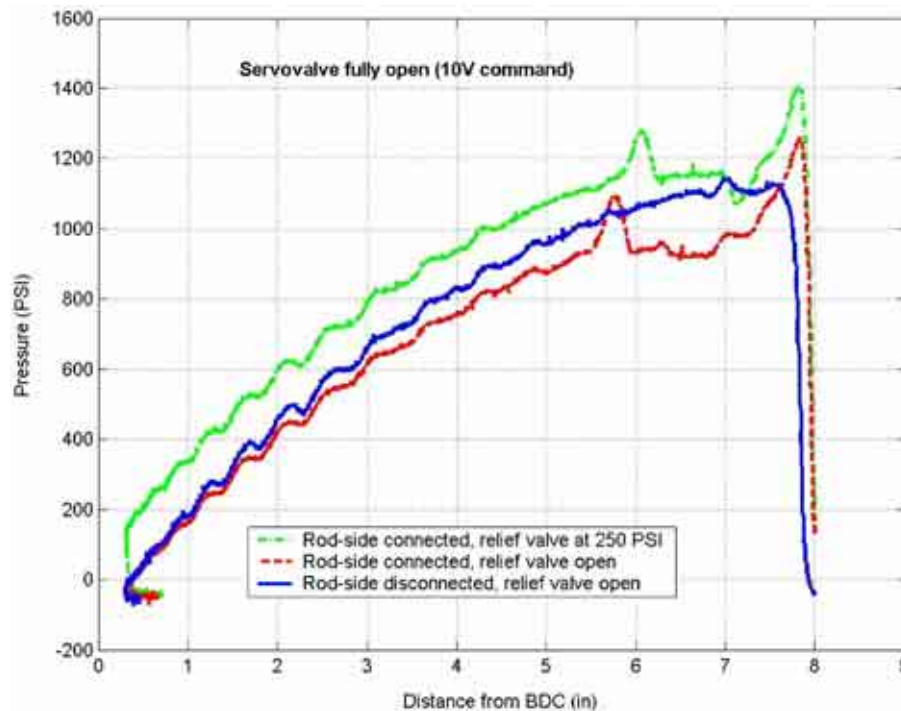


Figure 2. Open-loop pressure response showing pressure spikes due to rod-side flow.

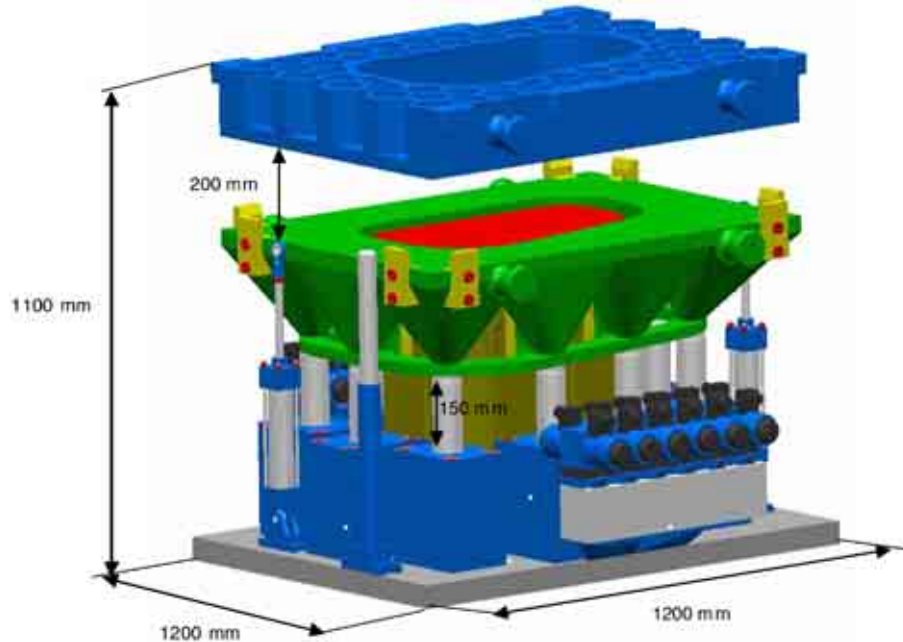


Figure 3. IFU binder control unit.

The closed-loop control system will automatically ensure that the desired binder forces are applied to the part by an electro-hydraulic actuation system during the forming process. The feedback control system will compensate for minor disturbances in the forming system caused by friction variation, inconsistent material properties, sheet thickness variation, die alignment problems, ram tilt, tool wear, blank placement, and press table deflection.

Feedback measurements will be used to modulate the binder force in real-time to keep optimum binder force trajectories for each cylinder in the control unit on target. The difference between the input signal and the output response will be fed to the controller to reduce the error and bring the output of the process to a desired value. One control strategy that can be used would have the following scenario:

- Finite-element method (FEM) produces an optimum material flow/friction trajectory.
- Sensor measures actual material flow/friction.
- Controller manipulates binder to achieve material flow/friction compliance.

In a closed-loop system, there is no need to determine in advance the binder forces needed to make a successful part because the system will modulate the forces based on measurements of the control parameter (material flow/friction).

IFU acquired the ten hydraulic cylinders, servo valves, and valve blocks; finished casting and manufacturing the punch, blank holder, die ring, and base plate for the Hishida die; acquired the sensors; and finished the development of the control system with the touch screen. The components are scheduled for assembly by the end of 2003, and unit testing is scheduled for the first quarter of 2004. The unit will be shipped to TDM in April for setup and testing in May–June of 2004.

### **Computer Simulation and Process Optimization Capabilities for Flexible Binders**

BHF plays a key role in the sheet stamping process by applying a restraining force on sheet material to suppress wrinkles and eliminate splits. Many studies have pointed out that blank holder profiles that

can be varied in time and in space increase the formability of the stamping parts. Two methods for predicting feasible/optimum variable BHF profiles, AS and OPT were applied to determine the variable BHF profiles.

AS is used in this study to “optimize” the stamping process by automatically adjusting the process parameters (i.e., BHF profiles) within a single FE simulation. The strategy in AS is to monitor/identify defects (i.e., wrinkle and split) and promptly correct them by adjusting the relevant process parameters during the simulation run.

OPT involves minimizing the value of a certain objective (also called cost) function, subject to some constraints (thinning and wrinkling limits). The objective function depends on parameters called design variables. The problem is to determine the value of these design variables so that the objective function is a minimum.

This study used AS and OPT to predict the variable BHF profiles for conical cups, rectangular pans, a tapered non-axisymmetric pan (Hishida part), and an S-rail. Experiments were also conducted to verify the predicted optimum BHF profiles.

### Conical Cups

Figure 4 shows a conical cup formed by optimum constant BHF of 26 tons (255 kN). The formed cup showed visible necking at a forming depth of 43 mm. Figure 5 shows a conical cup formed by optimum variable



**Figure 4.** Cup formed with optimum constant BHF. The cup showed visible necking at 43 mm.



**Figure 5.** Cup formed with optimum variable BHF. There is no visible necking at 47 mm.

BHF. The formed cup did not have any visible necking at a forming depth of 47 mm. This proves that optimum variable BHF profiles improve the formability of drawn cups compared with those drawn by optimum constant BHF profiles.

### Rectangular Pans from DP600

AS and OPT were also used to predict the optimum BHF profiles for rectangular pan drawing. Although the BHF profiles predicted by AS and OPT for pan drawing of 50- and 90-mm depths are different, they form good parts with almost identical thinning distributions. The results lead to the conclusion that the rectangular pan allows a large forming window. Considering the computation time required, in this case study, the application of AS to determine an optimum BHF profile seems to be more efficient than OPT.

AS requires only one simulation run to result in a feasible variable BHF profile; OPT needs many more iterative simulation runs to result in an optimum variable BHF profile. In this study, the BHF profile from AS was applied as an initial guess for OPT. The result was a reduced number of iterative simulation runs, which decreased the total computation time.

In view of the simulation results, these conclusions can be stated:

- AS and OPT successfully predicted feasible/optimum variable BHF profiles

for rectangular pan drawing. In the simulation, improvement was obtained on overall thinning distribution of the part formed with the predicted variable BHF profile compared with a part formed with a constant BHF (408 kN).

- Feasible BHF profiles predicted by AS can be used as initial guesses for OPT. This reduces the number of iterative simulation runs and decreases total computation time. The combination of AS and OPT can lead to prediction of optimum BHF profiles for general stamping parts with fewer simulation runs than required using OPT alone.

### Non-Axisymmetric Pans from AA5182-O and AA6111-T4

AS and OPT codes were updated to handle the IFU Hishida geometry for detecting sidewall and flange wrinkle. Constant and variable BHF profiles for the part were predicted using AS and OPT codes

coupled with FE modeling. Materials used were 1.15-mm AA5182-O and 1.0-mm AA6111-T4 aluminum sheets. The blank shape was selected based on experiments conducted at IFU. Figure 6 shows the dimensions of the blank and locations for monitoring sidewall wrinkles.

The FE model used for simulating the IFU-Hishida die drawing process with AA5182-O material is shown in Figure 7. The blank was modeled using free mesh with 4-node shell elements. The flow stress of the sheet material was obtained using tensile test and then curve-fitted to power law. ALCAN conducted the tensile tests for GM, which provided the material properties of the material. Hill's 1990 yield criterion was used in the FE simulations. The anisotropy constants in Hill's 1990 yield criterion were obtained using tensile test data and biaxial test data from literature. A coulomb friction coefficient of 0.08 was used at all the tool-sheet interfaces.

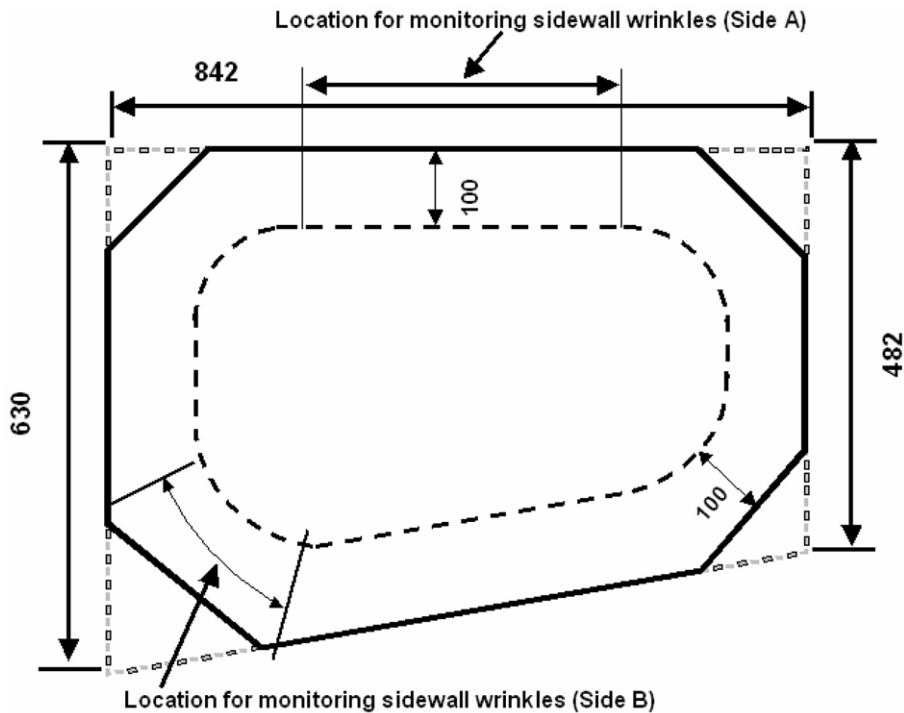


Figure 6. Dimensions of the blank used in the FE simulation and locations for monitoring sidewall wrinkles.

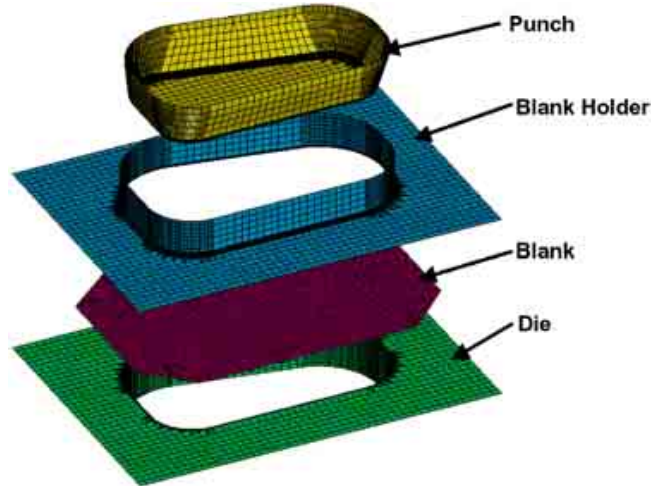


Figure 7. Schematic of the FE model used for IFU-Hishida die drawing simulations.

During FE simulation of the process, the BHF was varied using AS and OPT strategies to predict time varying and/or constant BHF profiles to form a given part with a desired quality (thinning and wrinkling). Currently, thinning and wrinkling are the only parameters used to monitor part quality. Wrinkling in the FE simulation is detected both in the flange and in the sidewalls. It was observed that the wrinkle amplitudes were more sensitive to BHF at the long sides of the pan than at the short sides and corners.

Thinning distributions along two sections were compared for the three different BHF profiles predicted by FE simulations: constant BHF obtained from OPT, variable BHF obtained from OPT, and variable BHF obtained from AS.

A comparison of thinning distribution obtained for three different BHF profiles along one section is shown in Figure 8. Results show that using variable BHF profiles results in a slight improvement in thickness distribution compared with constant BHF. The improvement could be due to the insensitivity

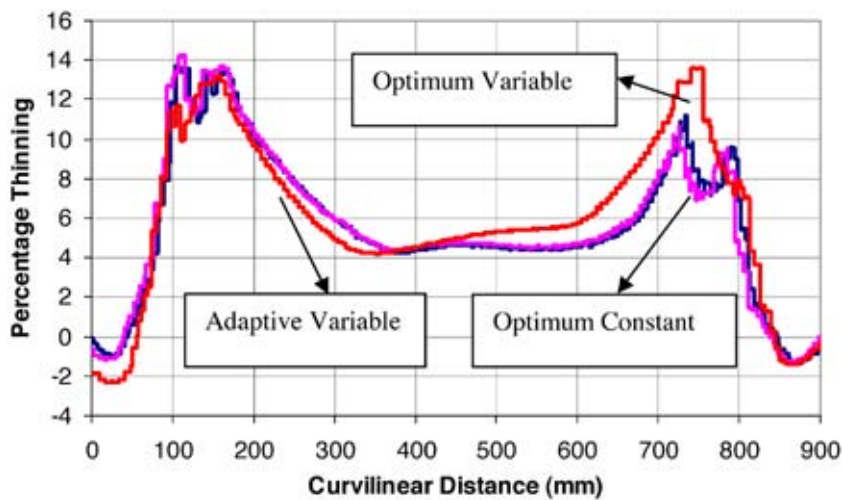


Figure 8. Comparison of thinning distribution predicted by FE simulation along a section for three different BHF profiles obtained from OPT and AS for AA5182-O.

of thickness variation to the time-varying BHF for this tapered pan geometry drawn to a height of 60 mm. Forming pans to a greater depth (greater than 60 mm) may show improvement in formability with the use of variable BHF.

Major conclusions drawn from the IFU-Hishida part study are these:

- Optimum constant and variable BHF were predicted using AS and OPT.
- Thinning decreased from 14.6% to 13.5% for variable BHF from AS compared with optimum constant for material AA5182-O.
- Thinning decreased from 13.5% to 12.0% for variable BHF from AS compared with optimum constant for material AA6111-T4.
- Optimum variable BHF did not improve formability for both the materials. More control points are needed in the B-spline to describe complex-shape BHF trajectories with compromise on simulation time. A variable BHF profile predicted by AS could be used to decide the number of control points and initial guess for OPT.
- Adaptive variable BHF resulted in slightly more uniform thickness distribution compared with optimum constant BHF.

- In this geometry, the effect of variable BHF (variations in stroke) was not significant, because little reduction in thinning was observed using variable BHF compared with constant.

## S-Rail

Springback is a major problem in the stamping industry, especially in high-strength and/or low-modulus materials such as aluminum alloys and high-strength steels. Locking the material during the final stages of the forming cycle has been shown to significantly reduce springback. Therefore, there is a need to determine optimal BHF profiles for stamping sheet metal parts.

AS and OPT techniques coupled with the FE method were applied to predict constant and time-varying BHF profiles for the S-rail to minimize springback in the part. The material used was 0.92-mm-thick AA6111-T4. The FE model used for simulating the S-rail part is shown in Figure 9. The blank was modeled using free mesh with 4-node shell elements. Material properties of the sheet material AA6111-T4 were obtained using tensile tests from GM. During FE simulation of the process, the BHF was varied using AS and OPT strategies to

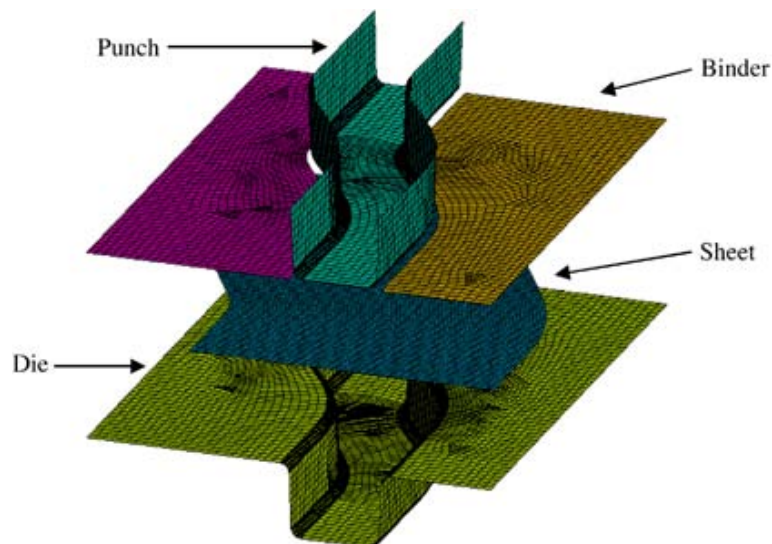


**Figure 9.** Schematic of the FE model used for the S-rail part simulations.

predict time-varying and/or constant BHF profiles to form parts with the desired quality (thinning and wrinkling) and minimum springback.

In this study, variable and constant BHF were predicted for the S-rail part for two cases:

- minimize thinning and avoid wrinkling without considering springback, and
- minimize springback and thinning and avoid wrinkling.

Wrinkling in the FE simulation was detected in both the flange and the side walls of the S-rail. Figure 10 shows the location of side wall wrinkles in the part simulation.

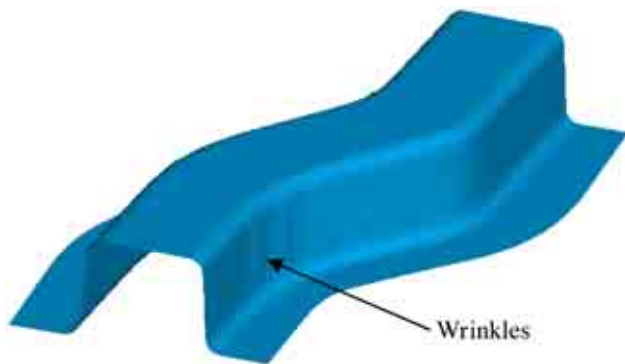


**Figure 10.** Location for side wall wrinkle monitoring in the S-rail part.

Results show that using variable BHF from AS resulted in a decrease in maximum thinning from 34% to 17% compared with the constant optimum BHF, although variable BHF from OPT resulted in a decrease in maximum thinning from 34% to 20% compared with constant BHF.

Major conclusions from the S-rail study are these:

- Optimum constant and variable BHF were predicted using OPT and AS with and without springback control.
- Springback in the part during forming was quantified using the ratio of the internal moment to internal force ( $v$ ) based on the mechanics of springback and results from past research. This ratio

was used in OPT and AS as an index for springback in the part.

- The 37-mm-deep S-rail part could not be formed without wrinkling and excessive thinning using constant and variable BHF profiles from AS and OPT. Beyond a depth of 32 mm, maximum thinning in the part increased rapidly and would result in failure. Therefore, the S-rail part of 30-mm depth was considered for further analysis to predict constant and variable BHF.
- Thinning decreased from 34% to 17% for variable BHF from AS without springback control compared with optimum constant without springback control for a 30-mm-deep S-rail part.
- Thinning decreased from 34% to 20% for optimum variable BHF from AS without springback control compared with optimum constant without springback control for a 30-mm-deep S-rail part.
- Two OPT methodologies were implemented to predict variable BHF that reduce springback in the part. For the S-rail geometry, variable BHF predicted by both the methods could not improve springback in the part because thinning in the part reached a maximum allowable limit of 20% even without springback control.
- Springback control based on post-stretching was implemented using AS. Post-stretching was initiated when the amount of stroke available ( $\lambda$ ) was equal to one-half of the die corner radius (2.5 mm). Variable BHF with springback control predicted by AS resulted in a 50% reduction in springback compared with variable BHF without springback control.
- Variable BHF from AS performed better than OPT because, in OPT, the shape of the curve is restricted by number control points used to generate the B-spline that represents the BHF. More control points in the B-spline would increase the complexity of the curve at the expense of computing time.

## **B. Warm Forming of Aluminum—Phase 2**

*Project Leader: Suresh Rama*

*DaimlerChrysler Corporation*

*2730 Research Drive*

*CIMS 463-00-00*

*Rochester Hills, MI 48309*

*(248) 838-5356; fax: (248) 838-5338; e-mail: scr4@daimlerchrysler.com*

*Project Administrator: Constance J. S. Philips*

*National Center for Manufacturing Sciences*

*3025 Boardwalk*

*Ann Arbor, MI 48108-3266*

*(734) 995-7051; fax: (734) 995-1150; e-mail: conniep@ncms.org*

*Technology Area Development Manager: Joseph Carpenter*

*(202) 586-1022; fax: (202) 586-1600; e-mail: joseph.carpenter@ee.doe.gov*

*Field Technical Manager: Philip S. Sklad*

*(865) 574-5069; fax: (865) 576-4963; e-mail: sklads@ornl.gov*

---

*Contractor: U.S. Automotive Materials Partnership*

*Contract No.: DE-FC05-02OR22910*

---

### **Objective**

- Develop and demonstrate a production process for the warm forming (WF) of aluminum for automotive body structures, and measure the economic feasibility of the WF process in a mass production environment.

### **Approach**

- Establish a warm-forming process in a laboratory environment with the application of new processes on a variety of aluminum sheet alloys. Balance alloy and lubricant development with continuing evaluation of commercial alloys, along with process modeling, design, and demonstration.
- Develop full-size demonstration of WF process and run tests in a production environment. Integrate a blank preheater, blank transfer mechanism, lubricant application system, WF press with a modified thermal profile controller, and lubricant removal step into production trials. Conduct production feasibility tests of the WF process at standard rates for current forming processes.
- Create a technical cost model that can generate cost comparisons between a warm-formed aluminum door inner and a same or similar door inner manufactured using conventional forming processes in steel and aluminum.
- Improve the formability of aluminum through development of enabling process advancements:
  - Establish the degree of improvement in formability of production-grade, commercial aluminum alloys.

- Develop a cleanable lubricant suitable for use in a WF process.
- Optimize the temperature distribution of the die.
- Evaluate rapid heating systems for blanks.
- Optimize the process design and layout.
- Apply the results of the cost model to optimize process design.
- Demonstrate the manufacturing feasibility and economic feasibility for a new mass production process such as the WF process.
- Define the process flow.
- Develop and apply a technical cost model that allows comparison of a product made in the WF process with a comparable component fabricated from aluminum/steel with deep draw using current processes.

### **Accomplishments**

- Completed the technical cost model and used model in current research work.
- Made progress toward identification of suitable aluminum material from candidate commercial alloys in laboratory-based WF process studies.
- Studied custom-formulated 5000 series aluminum alloys in laboratory formability tests in 2002 with inconclusive results.
- Used technical cost model data to show that material cost had highest impact on process costs. Therefore in 2003, formability studies were redirected to focus on commercially available 5000 series alloys to avoid the cost impact of expensive additives in custom alloys. WF process feasibility will be directly affected by the ability to use commercially available alloys.
- Made positive progress toward identification of a suitable lubricant through extensive laboratory-based studies.
- Made positive progress in the thermal analysis of the die through a heat transfer analysis of the WF dies to be used in the WF process scale-up. Objectives of this analysis include:
  - determine optimal (“good”) heater layout, spacing, and size to achieve optimum temperature distribution over the die surface,
  - determine consequent die distortion effect,
  - develop guidelines for heating scheme for WF tooling for practical use in mass production, and
  - identify process parameters through this model including the time necessary for the top insert surface to reach an average temperature suitable for WF; heat expansion of the insert top surface in width, height, and thickness; and the temperature/distortion change after heating step is complete.

### **Future Direction**

- Finish thermal studies and thermal models.
- Finish lubricant studies, and select the lubricant formulation for use in production demonstration.

- Investigate continuous cast aluminum materials for WF, compare to 5XXX series aluminum performance, and select an alloy for use in production demonstration.
- Decide on blank heating system to be used in production demonstration.
- Set up at contractor's site for production scale-up and demonstration.
- Employ the technical cost model to compare costs of WF process and alternative processes.

## **Introduction**

In a quest to improve fuel economy, the automobile manufacturers have been seriously looking at aluminum to lightweight their vehicles. Because aluminum costs more than steel and because most automotive-grade aluminum alloys have limited formability, a cost penalty is associated with their use. The challenges include

- transferring steel-based designs for aluminum due to reduced formability,
- sliver management in trimming aluminum panels,
- difficulty in forming sharp-edge contours,
- hard-to-achieve deeper draws, and
- appearance problems in most 5000-series aluminum panels.

Warm Forming of Aluminum, Phase 2, was initiated after the initial technical feasibility of forming complex shapes at elevated temperatures was demonstrated. It is a 4-year development and demonstration program to establish the "production" feasibility of WF aluminum alloy blanks into automotive panels, such as shown in Figure 1, and to fully demonstrate a WF



**Figure 1.** Dodge Neon door inner representing body panel with deep draw requirements.

process for cost-effectively manufacturing aluminum automotive panels with deep draw.

The main purpose of this project is to focus on the following objectives:

- Develop and demonstrate a WF process including the materials, equipment, and heating processes that can cost-effectively expand the forming limits of aluminum sheet.
- Develop a technical cost model for the WF process that will help assess the economic feasibility of the warm forming process specific to component design.

The major enabling process improvements to make WF a production-capable process are the following:

- use of a high-temperature lubricant that has good lubricity at WF conditions and also is easy to wash off for automotive painting,
- managing temperature distribution on the die surface during the forming operation,
- effective preheating methods for blanks, and
- any improvement in alloy chemistry for improving the sheet fabrication at material supplier to reduce costs.

## **Phase 2 Detail**

- **Technical cost model:** Camanoe Associates developed a very detailed cost model based on the process sequence agreed on by the project team. The sequence was established based on several discussions and data obtained from various testing from prior years. It was found that the

- material cost accounted for more than 70% of the cost of the product, and thus a new direction in alloy development/selection was identified.
- **Alloy selection:** In 2003, this task, which was assigned to the University of Michigan, focused on improving the sheet fabrication process for WF-capable aluminum sheet at reduced costs. Because material costs are the largest cost factor of a warm-formed part cost, the efforts at the University of Michigan were redirected toward analyzing the warm formability of commercially available alloys.
  - **Lubricant selection:** The performance of various lubricants under different temperatures was evaluated through two major test methods: Tribotester at General Motors and lab-scale WF of pans at the University of Michigan. Lubricant formulations and cleanability evaluations were conducted at Fuchs laboratories.
  - **Die thermal analyses:** University of Michigan's S. Wu Manufacturing Center is performing detailed finite-element analyses (FEAs) for investigating the temperature profiles on the stamping die and blanks for Neon door inners. Data about the geometry and heater locations on the die were obtained from computer-aided design (CAD) models of the die provided by Sekely Industries.
  - **Blank heating:** Preliminary evaluation of infrared (IR) heating for heating blanks was investigated at the University of Michigan. The results will assist the team in determining if IR or another heating method is the best preheat method for large volume production.
  - **Alloy fabrication:** With the focus on the investigation of warm formability of commercially available aluminum alloys, no additional custom alloys will be specified for fabrication by Pechiney Rolled Products. Pechiney continues to supply 5000 series aluminum sheet for these formability studies.
  - **Full-scale process demonstration:** Once the individual component processes are validated at laboratory level for technical and economic feasibility, a full-scale WF demonstration using the Dodge Neon door inner stamping dies will be conducted. The work is currently planned to be conducted at Sekely Industries in 2004, press time and other scale-up variables considered. Additional suppliers may be considered for participation in the system integration and process demonstration if their resources would allow a full-scale process demonstration inclusive of a material flow process.
  - **Postprocess inspection and material analyses:** Coupons from warm-formed parts will be cut out, and the materials properties will be evaluated by one of the original equipment manufacturers (OEMs). The typical properties to be evaluated will include strength, distortion, and corrosion.

## **Phase 2 Accomplishments**

**Technical cost model analyses**—At the start of the year, the WF Project core team, consisting of the representatives from DaimlerChrysler, Ford, and GM, reviewed the results of the technical cost model and redirected the course of research and development for 2003. The technical cost model was developed by Camanoe Associates. One of the main components of the cost model is the process sequence. The project team agreed on a process sequence that would be suited for a high-volume production WF process, including the process steps, blank lubrication, blank preheating, warm forming, and cleaning. Using straw-man example rates for labor, maintenance, and overheads, the technical cost model was shown to be able to generate a comprehensive cost breakdown for a Dodge Neon door inner panel if it were to be mass produced (250,000/year) using the identified WF process sequence.

The material cost accounts for more than 70% of the final product cost of the Dodge Neon door inner panel. Minimizing material cost in the WF process became critical. The original direction of developing new WF alloys by modifying the alloy chemistry of certain 5000 series alloys was only contributing more expense to the material cost component. Therefore, the core team decided to focus on commercially available 5000 series alloys, specifically 5182 and 5754 at oxygen and hydrogen tempers. It is desirable to add continuous cast sheet products to the alloy study if suitable material can be located at an economical price. Pechiney Rolled Products provided the project with the necessary amounts of 5182 and 5754 in both oxygen and hydrogen tempers.

**Blank preheating and IR heater studies**—The laboratory IR heater system was delivered to University of Michigan and integrated to work with the lab-scale WF press. The setup of the IR heater system included a control panel that later was modified to provide direct adjustable control over the conveyor belt speed. At this time, the distance between the heating lamps and the sheet is determined to be 5 in. since the entire system is 66 cm long, the heat loss from the inlet and exit of the heater is significant. Insulation at the entry and exit was added to contain the heat within the furnace so that the IR lamps can effectively heat the sheet (blank). Several tests were performed to study the effect of IR heat on WF process and microstructure.

Trials with the IR heater showed a relatively slow heat-up time. This is shown in Figure 2 where the time to heat the sheet to 300°C was approximately 3 min at an oven temperature of 400°C. To achieve production-level process times, a very long oven would be required for the blanks to reach the target temperature prior to reaching the press. This type of heater system would both be impractical and not cost-effective for the forming process.

In an effort to decrease heating time, several experiments were conducted at

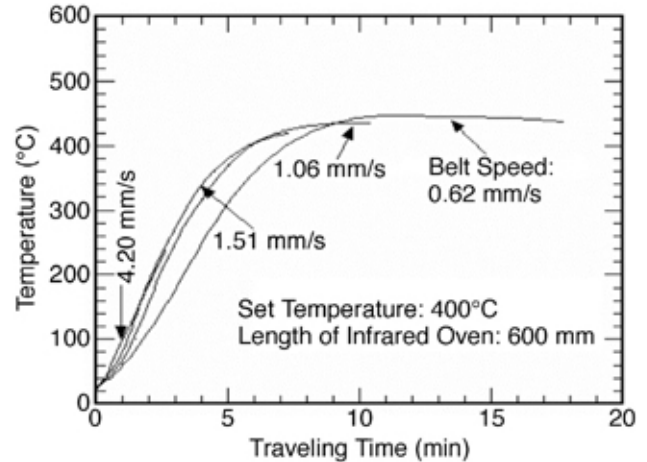


**Figure 2.** Sheet temperature as a function of time for three different belt speeds at an oven set temperature of 400°C.

higher set temperatures. The time vs temperature plots for heating trials at 800°C and 900°C are shown in Figures 3 and 4, respectively. Time to reach 300°C for these trials was closer to 35 and 25 s for the two oven set temperatures, respectively. This represents a significant improvement over the previous results at a set temperature of 400°C.

Photomicrographs of the material after heating to certain times indicate the materials become fully recrystallized at 76 and 50 s for the two set temperatures (see Figures 3 and 4). Recrystallization prior to forming is required to attain maximum formability. Material cost savings can be attained by using “hardened sheets” such as these instead of having the sheet batch-annealed at the aluminum manufacturing facility.

While these trials demonstrated that an IR oven is capable of supplying ample heating for the WF process, it does not appear to be the best solution. Significant overheating appears to be necessary to achieve production feasible heat-up times. Additionally, overheating presents the risk of melting the sheet if the conveyor system were to stop for any period of time. Additionally, highly emissive aluminum requires significant energy from the IR heater to reach target temperatures. For these reasons, the team decided to use a conduction heater, which is

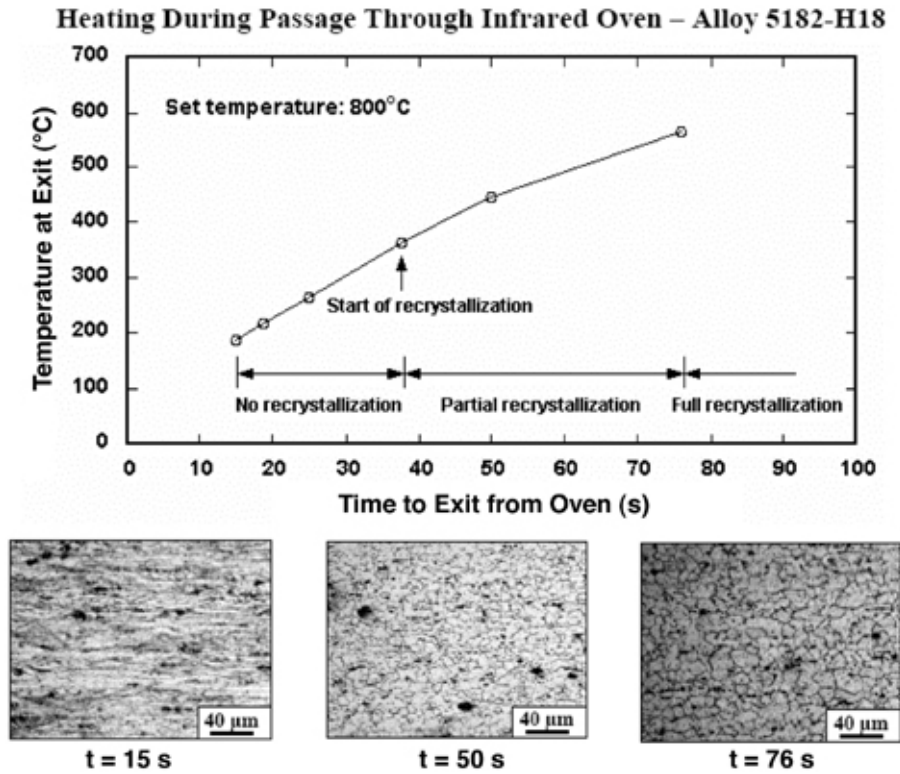


Figure 3. Sheet temperature as a function of time at an oven set temperature of 800°C. Note from the micrographs that full recrystallization occurs at approximately 76 s of heating time.

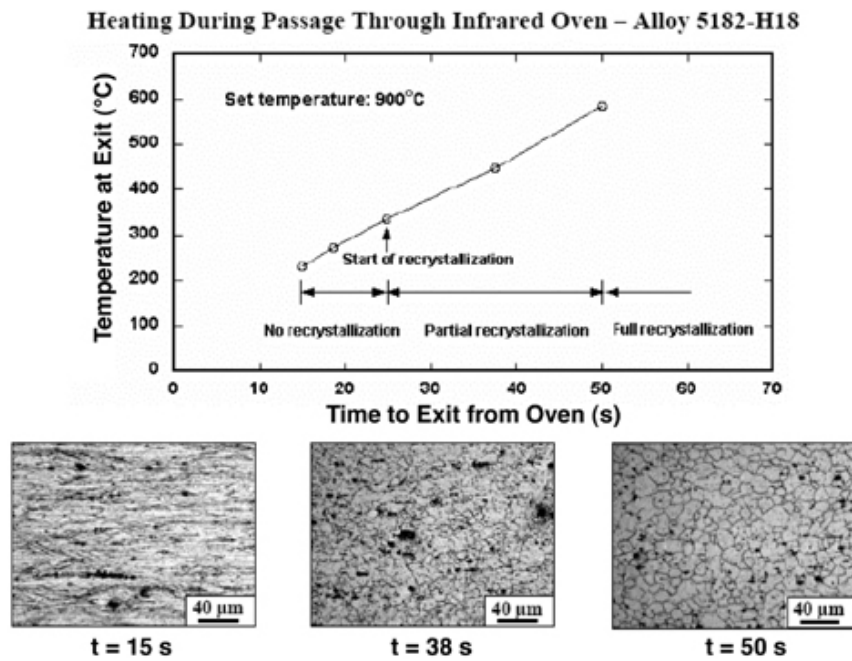


Figure 4. Sheet temperature as a function of time at an oven set temperature of 900°C. Note from the micrographs that full recrystallization occurs at approximately 50 s of heating time.

thought to be a more cost-effective and robust method of heating aluminum sheet, in the scale-up of the WF process. Preliminary tests indicate that forming temperatures can be reached within seconds with this type of heater.

**Lubrication studies**—Lubrication formulations and their effect on the formability of aluminum under various temperatures were studied by Fuchs Lubricants and GM. GM and Fuchs previously completed formability tests using Fuchs LN1184 and LN1169 lubricants at 215°C, 260°C, and 315°C, examining the lubricant layer after forming, drawing behavior due to lubricant/temperature effectiveness, and length of the wear scar and compared these test results with results of dry forming. Findings confirmed that cup depths are a function of temperature and lubricant. Higher formability is found with some lubricants at certain temperatures, but cleanability can be worsened at increased temperatures. See Figure 5 for a visual of the cleanability issues posed by a lubricant.

In 2003 Fuchs performed room temperature screening of several new candidate lubricants, and GM performed high-temperature testing. Cleanability is still a major issue in lubricant selection. The experimental setup at the University of Michigan used for the studies conducted by GM is shown in Figure 6.



**Figure 5.** Lubricant cleanability issues postforming at varying temperatures readily apparent on these sample parts.



**Figure 6.** Punch and die setup at University of Michigan for lubricant studies conducted by GM.

Lubricant work then focused on trying to improve other previously developed lubricants produced by Fuchs. These included the following:

- SJA216 Base—thermally stable soap with a wetting agent,
- SJA216 BN—SJA216 Base + BN as solid lubricant, and
- SJA216 LN—Previously tested LN1184 + BN as solid lube.

These lubricants were evaluated using the following methods:

- pin on disc friction test at room temperature at Fuchs,
- cleanability testing after thermal exposure at Fuchs,
- ring on plate tribotester at GM under two temperature conditions, 250°C and 350°C, and
- pan die forming at University of Michigan at three preheat temperatures, 215°C, 260°C, and 315°C.

Two important results from this work follow.

The results shown in Figure 7 demonstrate that for the base lubricant, the coefficient of friction decreased with increasing temperature. More importantly, the addition of BN to the base lubricant increased the coefficient of friction. The BN additions were made anticipating a reduction in coefficient of friction and improved elevated temperature stability. Neither effect was observed in the present study. This suggests that different additions such as graphite and molybdenum disulfide might be better for this application.

The pan die forming results are summarized in Figure 8. These results again show that the addition of BN to the base lubricant decreases the effectiveness of the lubricant, in this case by decreasing the forming depth achievable at each temperature. There appears to be an optimum forming temperature around 250°C; however, the heating time and forming time (2–3 min) were longer than would be expected for a production system. This difference could lead to breakdown of the lubricant prior to forming and thus give a lower pan depth.

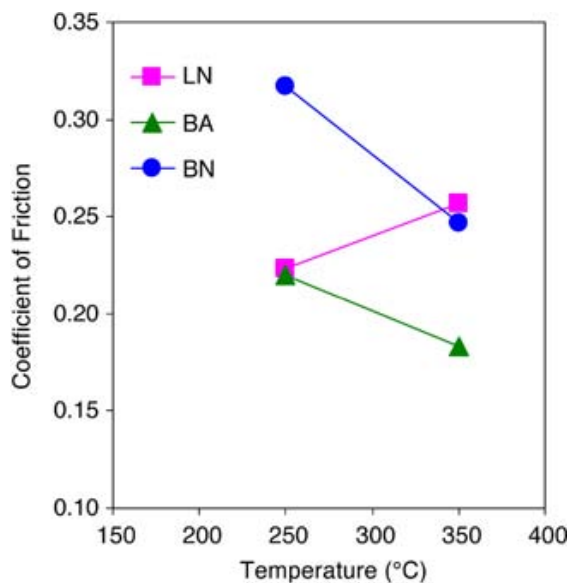


**Figure 7.** The effect of temperature on coefficient of friction during ring on plate tribotesting in three different lubricants. Plate material AA5083.

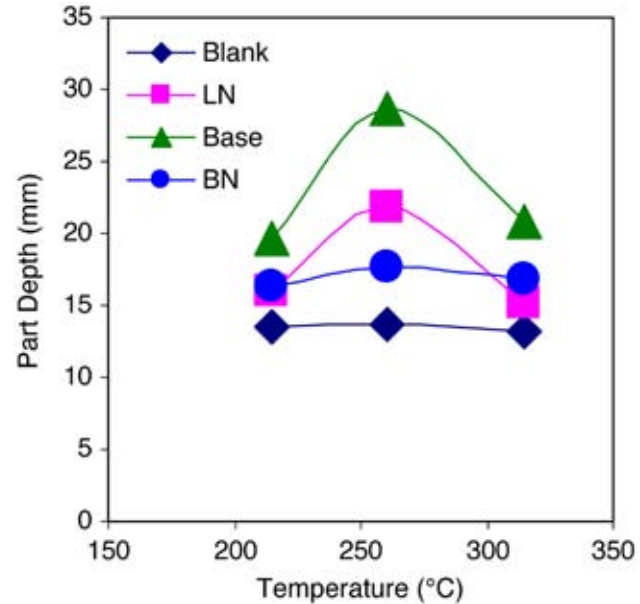


**Figure 8.** The effect of temperature on the pan die forming depth for a variety of lubricant systems.

This inconsistency in preheat and forming time can also explain why the friction coefficient data in Figure 7 showed the coefficient of friction decrease with increasing temperature; the data in Figure 8 show a reduction in formability with increasing temperature.

In 2004 lubricant studies will continue to evaluate alternate additives to the Fuchs base material, rapid preheating with the IR furnace to better control the thermal cycle in the process, valuation of the lubricants using a novel friction testing system at Ford, and evaluation of selected lubricant(s) on large-scale forming trials.

**Die and blank thermal analyses**—Positive progress has been made in the thermal analysis of the WF dies through a heat transfer analysis of the dies to be used in the WF process scale-up. A preliminary FEA model to study the heat-up and cooling of formed parts and die components was defined by S. M. Wu Manufacturing Research Center, University of Michigan. The FEA model was then used to examine the effects of air vs water cooling on simple deep draw parts, the loss of temperature during sheet material transfer from preheater to die, and heat

distortion effects on die and insert surfaces over time. Such information will be considered in the final process layout design.

Six parts (insert, low holder, blank, upper holder, punch, and base) make up this complex die-punch process. Heat fluctuation values for the die upper holder and insert were determined by a preliminary die heat transfer study. As part of this study, a three-dimensional sectional analysis of the die was done, and a simulation of the full stamping process was made.

Figure 9 graphically depicts the simulated process as well as the components of the die tooling and the thermal profiles of the tooling during the different WF process steps.

Blank distortion due to die thermal variances was also studied. The applied heat flux on the die during the heating stage caused die expansion. This expansion irregularity on the die surface was relatively small, and further expansion of the die during processes after heating was negligible. The formed

blank continuously shrank due to spring-back for 27 h (see Figure 10).

**Technical cost model completion—** Iterative versions of the strawman cost model were reviewed during this report period. Various views of product and process cost can be generated by the model, including graphical displays; this feature allows flexibility in process design, materials selection (end product and process), labor, energy, machinery/equipment, tooling, overhead elements, facility and maintenance costs. Figures 11 and 12 contain two output

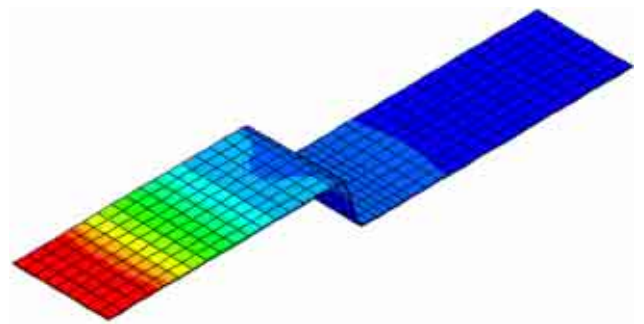


Figure 10. Blank deformation after WF.

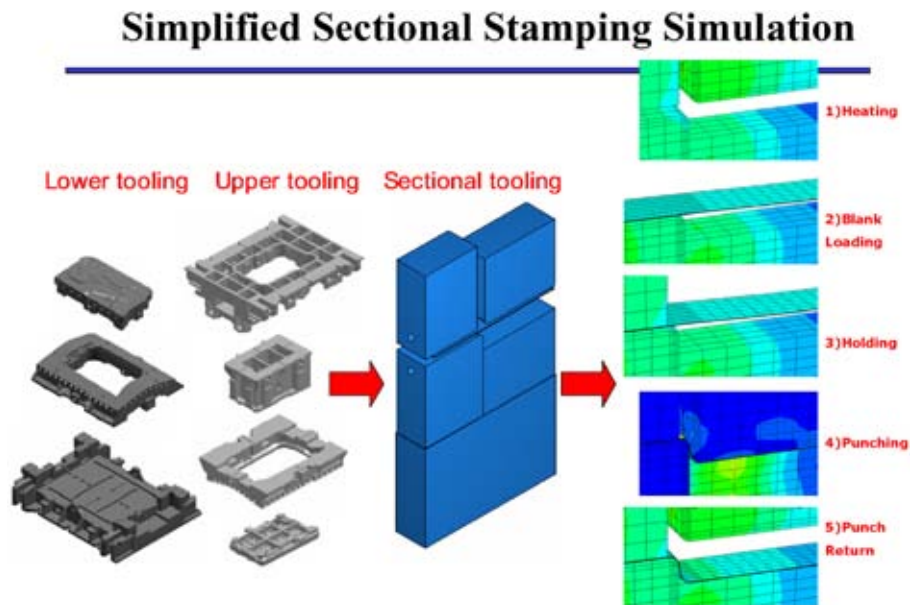


Figure 9. Dodge Neon door inner panel stamping die components sectioned and profiled to show thermal and vertical displacement data.

Breakdown by Cost Element		
Material	\$21.66	74.8%
Process Material	\$1.36	4.7%
Labor	\$1.17	4.1%
Energy	\$2.08	7.2%
Main Machine	\$0.92	3.2%
Tooling	\$0.81	2.8%
Overhead Labor	\$0.65	2.2%
Building	\$0.13	0.4%
Maintenance	\$0.19	0.6%
<b>TOTAL</b>	<b>\$28.98</b>	

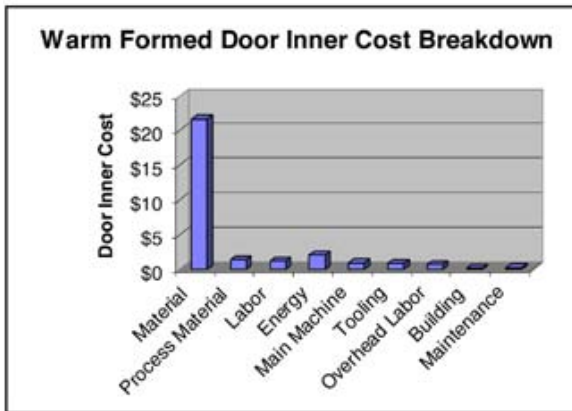


Figure 11. Example product cost display using strawman data inputs.

Breakdown by Process Step		
Material	\$21.66	74.8%
Blanking	\$0.79	2.7%
Lubrication	\$0.82	2.8%
IR Heating	\$1.20	4.1%
Forming	\$2.43	8.4%
Cleaning	\$2.07	7.1%
<b>TOTAL</b>	<b>\$28.98</b>	

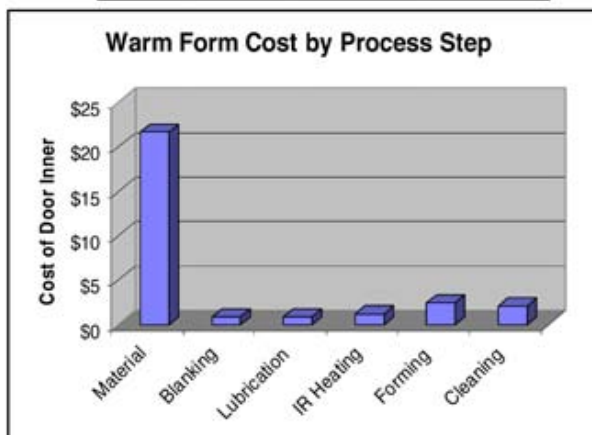


Figure 12. Example process cost display using strawman data inputs.

examples showing part and process costs in table and graphic forms. Strawman example data were used to generate these data for sample presentation purposes. The individual OEMs are now able to apply the technical cost model in their own proprietary planning using their confidential data as inputs. OEM confidential data and proprietary use of the technical cost model will not be shared among the team.

### Future Work

- Finish thermal studies and thermal models of the entire die to gain a better understanding of what temperature set points need to be maintained for a more uniform temperature distribution on the die surfaces.
- Perform additional lubricant studies and finalize the formulation options with limitations identified through laboratory testing and scale-up demonstrations.
- Investigate the WF of continuous cast aluminum sheets, and additionally, magnesium sheet formability using the same process infrastructure.
- Finalize the blank heating system specification to be used in production scale-up and demonstration.
- Set up at contractor's site for production scale-up and demonstration.
- Apply the technical cost model to generate costs for comparing the WF process with known alternative processes using the strawman format.

## C. Electromagnetic Forming of Aluminum Sheet

*Richard W. Davies, Principal Investigator*

*Pacific Northwest National Laboratory*

*P.O. Box 999, Richland, WA 99352*

*(509) 376-5035; fax: (509) 376-6034; e-mail: rich.davies@pnl.gov*

*Sergey Golovashchenko, Technical Coordinator*

*Ford Motor Company*

*Ford Research Laboratory, Dearborn, MI 48121-2053*

*(313)-337-3738; fax: (313) 390-0514, email: sgolovas@ford.com*

*Technology Area Development Manager: Joseph A. Carpenter*

*(202) 586-1022; fax: (202) 586-1600; e-mail: joseph.carpenter@ee.doe.gov*

*Field Technical Manager: Philip S. Sklad*

*(865) 574-5069; fax: (865) 576-4963; e-mail: skladps@ornl.gov*

### *Participants*

*Vladimir Dmitriev, EMF R&D, Ford Motor Company*

*Dwight Rickel, EMF System Development, Los Alamos National Laboratory*

*James Sims, Coil Durability, Materials, and Design, Los Alamos National Laboratory*

*Andy Sherman, EMF R&D, Ford Motor Company*

*Jeffrey Johnson, EMF System and Control, Pacific Northwest National Laboratory*

*Gary Van Arsdale, EMF System Design and Metal Forming, Pacific Northwest National Laboratory*

*Nick Bessonov, EMF Simulations, University of Michigan–Dearborn*

*Nick Klymyshyn, Computational Mechanics, Pacific Northwest National Laboratory*

*Dick Klimisch, Project Coordinator and Material Supply, Aluminum Association*

*Roy Cooper, Oxford Automotive Company, EMF Industrial Embodiment*

---

*Contractor: Pacific Northwest National Laboratory*

*Contract No.: DE-AC06-76RL01830*

---

### **Objective**

- Develop electromagnetic forming (EMF) technology that will enable the economic manufacture of automotive parts made from aluminum sheet.

### **Approach**

- Establish analysis methods for forming system design.
- Develop durable actuators (coils).
- Analyze industrial embodiment of the EMF process.

### **Accomplishments**

- Completed a literature search for information on EMF, coil materials, and coil design/durability.

- Completed design and assembly of a 150-kJ pulsed power unit (Figure 1) at Los Alamos National Laboratory (LANL).
- Tested Ford Motor Company's integrated forming coil system for high-volume automotive stamping.
- Used LANL's literature review of patents, relevant coil materials, and the design of EMF coils.
- Installed the 150 kJ pulsed power supply at Pacific Northwest National Laboratory (PNNL), demonstrated operation, and installed automated computer control system capable of automated cyclic testing and sheet metal forming.
- Completed fabrication of an experimental apparatus to evaluate coil durability.
- Established a Cooperative Research and Development Agreement (CRADA) that includes Ford, PNNL, and Oxford Automotive.
- Performed cyclic testing of an EMF coil assembly for durability assessment and achieved more than 1400 cycles.
- Developed conceptual layouts for industrial embodiment of EMF process.
- Demonstrated ability to improve formability of aluminum sheet by a factor of 2–3 times over conventional forming.

### Future Direction

- Increase the cyclic testing rate to better evaluate the thermal characteristics of the current industrial coil assembly.
- Continue to evaluate the durability of the Ford-PNNL coil assembly design through high-rate cyclic testing.
- Further develop modeling capabilities that can assist in the design of EMF systems.
- Continue to investigate the industrial embodiment of EMF systems for automotive manufacturing.

---

### Introduction

In the EMF process, a transient electrical pulse of high magnitude is sent through a specially designed forming coil by a low-inductance electric circuit. During the current pulse, the coil is surrounded by a strong transient magnetic field. The transient nature of the magnetic field induces current in a nearby conductive workpiece that flows opposite to the current in the coil. The coil and the workpiece act as parallel currents through two conductors to repel one another. The force of repulsion can be very high—equivalent to surface pressures on the order of tens of thousands of pounds per square inch. Thin sheets of material can be

accelerated to high velocity in a fraction of a millisecond.

A recent interest in understanding the EMF of metals has been stimulated by the desire to use more aluminum in automobiles. The high workpiece velocities achievable using this forming method enhance the formability of materials such as aluminum. Also, the dynamics of contact with the forming die can help reduce or mitigate springback, an undesired effect that cannot be avoided in other forming techniques such as stamping. The commercial application of this process has existed since the 1960s. The large majority of applications have involved either the expansion or compression of cylinders (tubes). The forming of sheet

materials is considerably more complex and has received relatively little attention.

### **Project Deliverables**

At the end of this program, methods and data to assist the economical design of EMF sheet forming systems will be documented. This will include (1) materials information and design methods for durable coils, (2) coil durability test data for selected materials and design concepts, (3) dynamic and hybrid formability data, (4) methods for modeling the forming process, and (5) concepts for the industrial implementation of the technology in an automotive manufacturing environment.

### **Approach**

This project will address three main technical areas. The first technical area involves establishing analysis methods for designing forming systems. These methods will be based on developed knowledge of forming limits and relations between electrical system characteristics and deformation response for specific aluminum alloys of interest. The second area of technical challenge is coil durability. Existing knowledge of EMF and relevant knowledge from pulsed power physics studies will be combined with thermo-mechanical analyses to develop durable coil designs that will be tested experimentally. Until a more thorough understanding is achieved of economic factors determining required durability, a nominal level of 100,000-cycle coil life will be the goal for this project. The third technical area involves the industrial embodiment of the EMF process. In this project, EMF is expected to be hybridized with conventional sheet metal stamping. Different approaches to hybridization will be analyzed for issues affecting economical implementation in a modern stamping plant. Different system concepts will be developed and studied. Existing knowledge of the EMF process and technical achievements in this project will be combined to

establish a methodology for designing hybrid forming systems that can be readily integrated into modern manufacturing facilities for the economic production of automotive sheet aluminum components. Some of the project focus areas and results are discussed in the following sections.

### **EMF System Commissioning**

Initial testing and trials of the new EMF system at PNNL were conducted in September and October 2001. The trials consisted of assembling the new EMF power supply system, load cables, and inductive load coil. The apparatus used to conduct the experiments is illustrated in Figure 1. The figure shows the four parallel coaxial conductors connected between the power supply and the EMF coil. Figure 2 is an enlarged view of the single-turn coil. The coil used was a single-turn, low-inductance aluminum alloy coil made from AA6061-T6. Also shown in Figure 2 are multiple sheets of Mylar sheeting and G10 (glass fiber composite) insulating materials. Not shown in the figure are the coil containment shroud and associated supports. The experiments involved multiple cycles of charging and discharging of the capacitor bank through the load coil at various known energy levels. The capacitor bank was controlled via the custom system developed for the unit. The



**Figure 1.** Photograph of the capacitor bank and load cables connected to the forming coil.

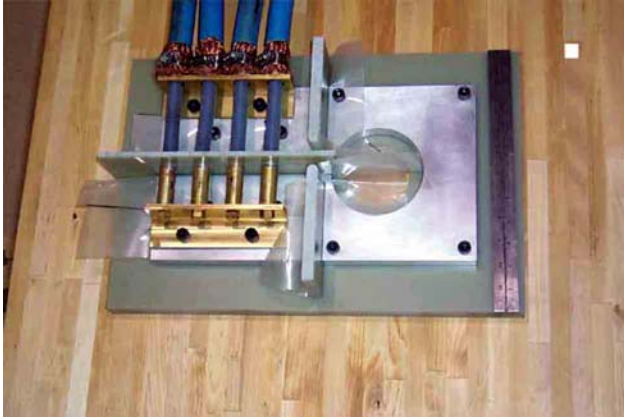


**Figure 2.** Photograph of the single-turn forming coil and the load cable connections.

sequence of testing consisted of charging the capacitor bank, isolating the charging power supply, triggering (releasing) the capacitor charge, and monitoring the response of the system. The system response was recorded using a high-speed digital oscilloscope. Figure 3 illustrates the typical response of the system during a 15-kJ discharge of the capacitor bank. This figure shows that the half-current (measuring half the total system current) of the system is approximately 86 kA, so that a total current of approximately 172 kA passed through the load

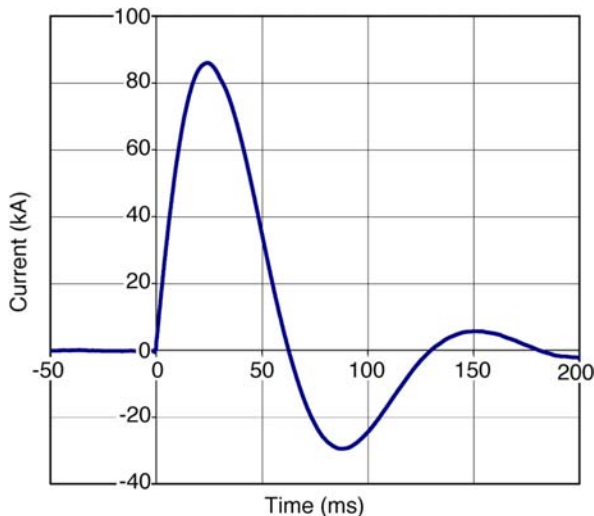


**Figure 3.** The current waveform that resulted during the initial system trials at PNNL. System charged to ~15 kJ, single turn coil, no ring suppression, half current plotted.

coil. The system rise time was shown to be approximately 26 ms. This EMF system has been commissioned and demonstrated with an automated cyclic testing during sheet metal forming. During the first half of FY 2003, the EMF capacitor bank has been demonstrated at current levels in excess of 225 kA. The system has also been cycled several thousands times at high current levels, while supporting our coil durability experimental work. The custom-designed control system was also successfully demonstrated in automated cyclic loading operating modes.

### Coil Design Concepts and Durability

During EMF, the high-intensity electromagnetic forces are applied to the turns of the coil. The coil, insulators, and support structure must resist these forces, as well as related thermal cycles, without significant permanent deformation or material failure. In contrast to typical cylindrical coils, sheet forming will require coils with general three-dimensional (3-D) shapes that are inherently less resistant to forces induced during forming. The key issues involve materials selection and design. Materials must be selected for both electrical conductivity and mechanical properties, and they must lend themselves to manufacturing. Materials may also need to be compatible with the presence of coolants and the forces generated during hybrid forming that combine conventional stamping and EMF. The design must integrate these elements, while delivering the primary function of a spatial and temporal load distribution that achieves the desired deformations. Coil systems will have to be low-cost, modular, and durable (nominally 100,000 cycles) if they are to be relevant to automotive manufacturing.

During the second quarter of FY 2002, LANL generated a technical report containing a conceptual coil design to perform in a high-volume manufacturing system. This particular design is considered modular and would likely require multiple coils to execute

any singular forming operation. This modular coil approach may require further study of coil-to-coil interaction and durability before it can be commercially implemented. In contrast, Ford Motor Company designed an integrated forming coil system for high-volume automotive stamping of complex components. This Ford-designed system has evolved into the system currently being tested for high-cycle forming trials at PNNL. This design integrates features that enhance the stiffness and durability of the coil during cyclic forming operations.

Beyond these trials on the Ford-designed coil system, PNNL has developed a system to evaluate these potential coil materials under high-cycle EMF conditions. PNNL has designed and fabricated a coil durability test apparatus, which was used early in the project for EMF testing. Figure 4 is a photograph of the coil configuration that is part of the apparatus (copper alloy shown). Removed from this coil photograph (for clarity) are insulating sheets of Mylar that retard cross-coil sparking. This coil is connected to the EMF capacitor bank and control system via cables that connect on the bottom side of the coil shown. This coil is designed to be placed in close proximity to a stationary aluminum alloy plate and subject to cyclic pulse loading at different power

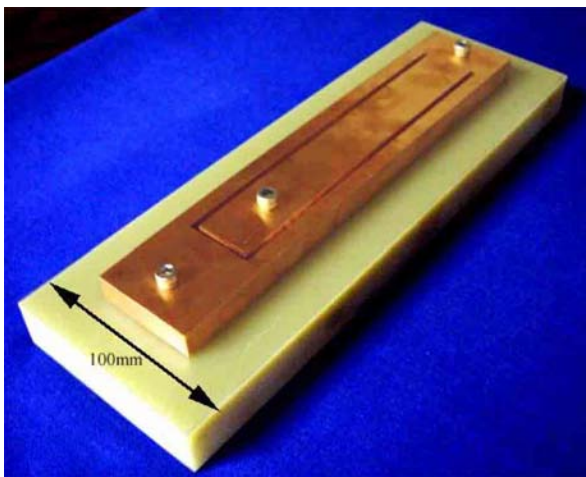


**Figure 4.** Photograph of the coil system originally used for testing different candidate coil materials.

levels and frequencies to determine the number of cycles to failure. The objective was to make coils from multiple materials and compare the coil durability across several samples from each population. This early work has evolved into testing of a full-scale coil assembly at PNNL.

### Coil Durability Experiments

During the first half of FY 2003, PNNL evaluated the performance of the latest coil assembly designed and fabricated under this project. The experiments consisted of evaluating the forming effectiveness, measuring the coil's thermal characteristics, and starting durability tests under cyclic loading of the coil system. Figure 5 shows a photograph of the Ford- and PNNL-designed coil assembly. Figure 6 shows photographs of the forming die used and the resulting formed aluminum sheet after testing. In this figure, the coil is directly below the aluminum sheet and the holes in the die are 3 in. in diameter. After a single EM pulse through the coil, the system forms three domes as shown in Figures 6 and 7. These forming experiments were conducted to learn the necessary pulse magnitude to effectively form aluminum

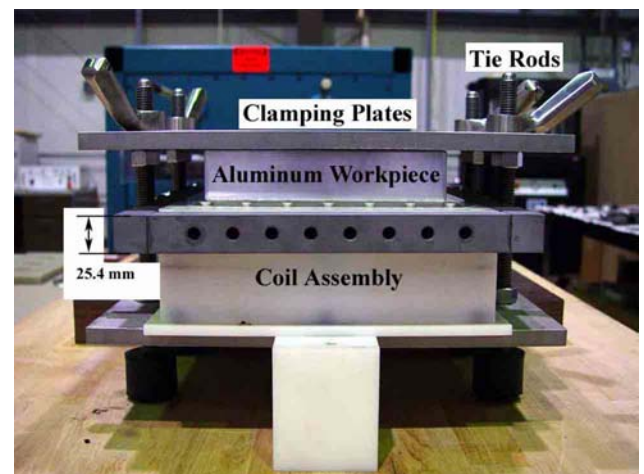


**Figure 5.** Photograph of the Ford- and PNNL-designed coil assembly. This assembly is currently undergoing cyclic testing at PNNL and has achieved more than 1400 cycles with no signs of coil degradation.

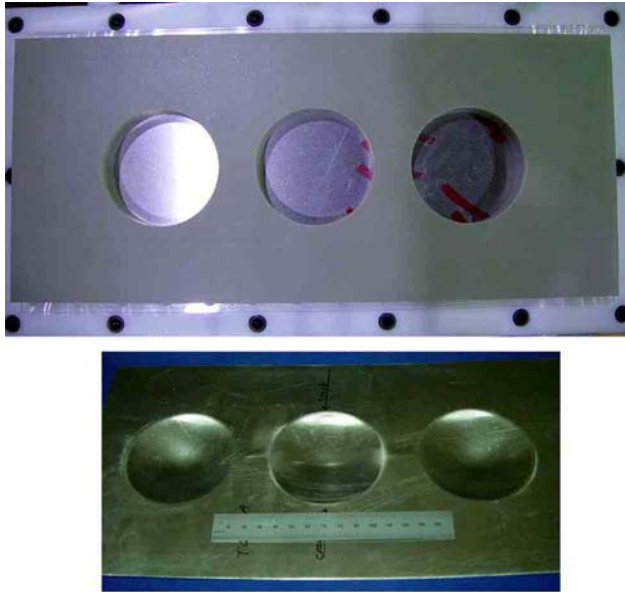


**Figure 6.** (top) Top view of the glass fiber-reinforced plastic tooling on the coil assembly with aluminum sheet metal between the coil and the tool. (bottom) Photograph of the deformed sheet after one EMF pulse through coil.

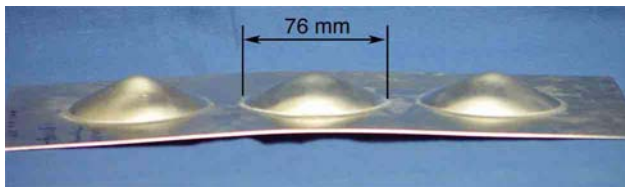


**Figure 7.** A formed aluminum sheet after a single EMF operation.

sheet. Subsequent to determining this critical EM pulse magnitude, PNNL initiated cyclic loading experiments on the coil system to determine the thermal and mechanical characteristics of the coil assembly to determine long-term durability. This assembly, which is currently undergoing cyclic testing at PNNL, has achieved more than 1400 cycles with no signs of coil degradation. These experiments are ongoing.

**Formability of Aluminum during EMF**

Ford Motor Company has conducted laboratory experiments to investigate the formability of aluminum alloy sheet during EMF. These laboratory experiments included

free forming of domes and forming of sheet metal into v-shaped die cross-sections. Figure 8 includes a cross section through a v-shaped forming die showing the coil, die, and the workpiece before and after deformation. This figure also shows the results of a typical strain grid analysis and the two to three times improvement in formability under these forming conditions. However, the experimental data have shown that the formability is sensitive to the shape of the die being used to evaluate the formability. Further investigation may be required in this area to better define the forming limits of the material under the varying biaxial and triaxial states of stress that develop during EMF.

**Numerical Simulation of EMF Process**

The EMF process is challenging to simulate because of the need to simultaneously model electromagnetic, thermal, and elastic-plastic deformation of materials. Many of the commercial research codes have serious limitations as well as an inability to accurately predict the results of EMF processes. This project has focused on integrating portions of existing commercial research codes to accurately predict the important characteristics of a 3-D EMF process. The current work involves collaboration with Dr. Bessonov in cooperation with the University of Michigan at Dearborn. Figure 9 illustrates an example of a two-dimensional simulation of EMF of aluminum sheet into a conical die with a fully coupled electromagnetic-elastic plastic model. These models are currently being extended for use as a fully 3-D numerical simulation approach. This work is ongoing.

**Industrial Embodiment**

Oxford Automotive is conducting an ongoing study into the industrial embodiment of the EMF process, which is designed to analyze the potential methods to incorporate EMF into the highly integrated manufacturing of automobiles. The study is investigating integration into conventional sheet

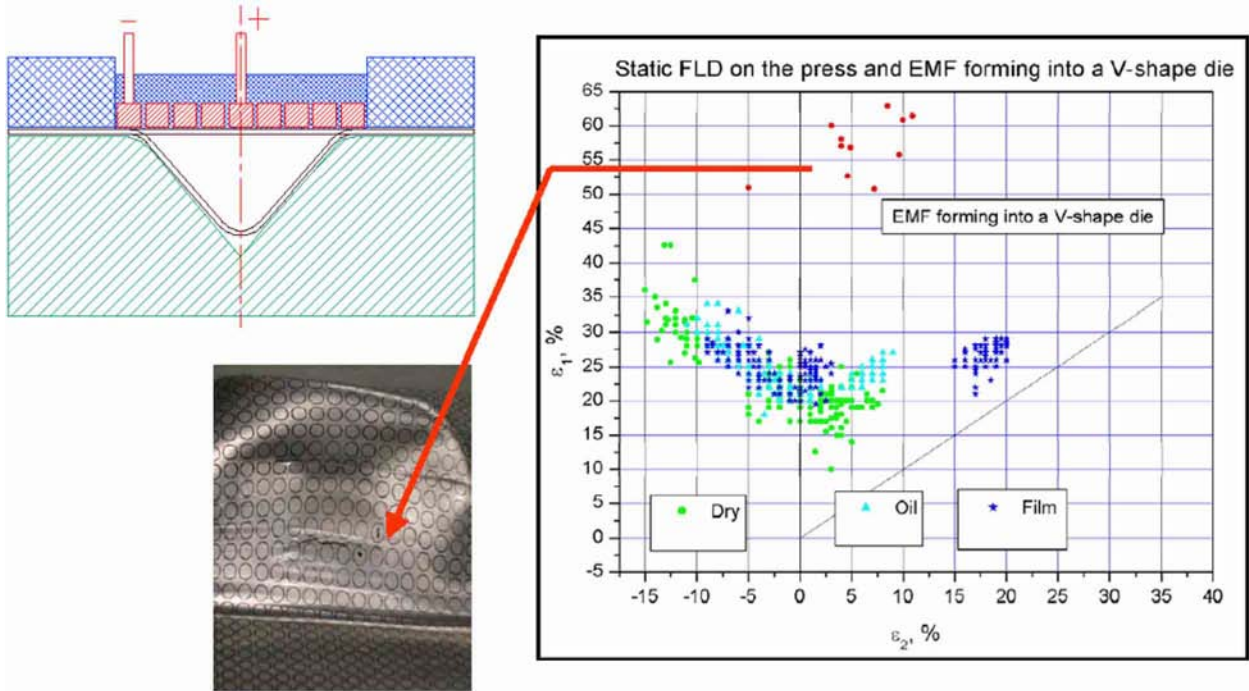


**Figure 8.** (Upper left) A cross-section through a v-shaped die showing the coil, die, and workpiece before and after deformation. (right) Strain grid formability data showing the improvement in aluminum formability under these forming conditions.

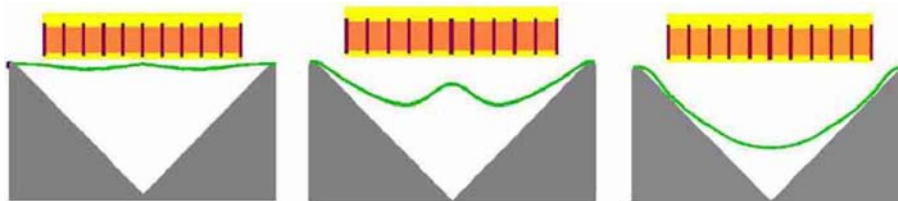


**Figure 9.** Example of a two-dimensional simulation of EMF of aluminum sheet into a conical die with a fully coupled electromagnetic-elastic plastic model. *Source:* Produced by Dr. Bessonov in cooperation with University of Michigan–Dearborn.

metal stamping production facilities and the potential to create an entirely new and separate production line based on EMF technology for aluminum alloy sheet. To date, several variations have been identified and are currently undergoing detailed study. Figure 10 shows a conceptual industrial embodiment of the EMF process as produced by Oxford. The system shown involves an EMF station located in conjunction with conventional mechanical presses. In the

scenario shown in Figure 10, the EMF system would be used as a separate forming station to perform a restrike function. This restrike operation would be employed to increase deformation in local regions that require greater formability than conventional stamping will permit.

### **Conclusions**

Technical feasibility of EMF for aluminum sheet in an automotive application has

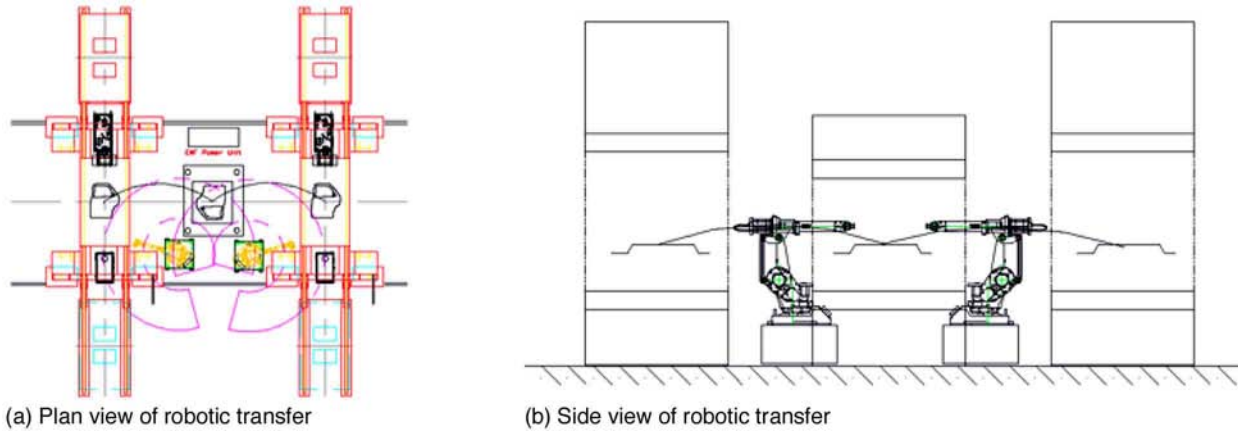


**Figure 10.** Conceptual industrial embodiment of the EMF process. The system shown involves an EMF station located in conjunction with conventional mechanical presses.

been demonstrated, during both this project and prior U.S. Council for Automotive Research projects. The durability of relevant coils systems and methods for the economical design, construction, and implementation of forming systems are yet to be demonstrated. There is also a need for additional dynamic formability data for relevant aluminum alloys. This project targets these issues. Progress has been made in assessing the current state of knowledge for materials, coil design, formability, and system design. Also,

a pulsed power system has been designed and fabricated to serve in experimental testing of coil systems. This project has also shown that EMF can be performed using aluminum sheet while achieving intermediate coil life (~1400 cycles). As this project progresses, a balanced combination of analysis and experiment will be applied to demonstrate more durable coil systems that meet the performance requirements of automotive manufacturing.

## **D. Aluminum Automotive Closure Panel Corrosion Test Program**

*Project Co-Chair: Tracie Jafolla*

*General Motors Corporation*

*Mail Code 483-370-101*

*3300 General Motors Road*

*Milford, MI 48380-3726*

*(248) 676-7014; fax: (248) 685-5279; e-mail: tracie.l.jafolla@gm.com*

*Project Co-Chair: Greg Courval*

*Alcan International*

*P.O. Box 8400*

*Kingston, Ontario K7L 5L9*

*(613) 541-2233; fax: (613) 541-2134; e-mail: greg.courval@alcan.com*

*Technology Area Development Manager: Joseph Carpenter*

*(202) 586-1022; fax: (202) 586-1600; e-mail: joseph.carpenter@ee.doe.gov*

*Field Technical Manager: Philip S. Sklad*

*(865) 574-5069; fax: (865) 576-4963; e-mail: skladps@ornl.gov*

---

*Contractor: U.S. Automotive Materials Partnership*

*Contract No.: DE-FC05-02OR22910*

---

### **Objective**

- Develop a cosmetic corrosion test for finished aluminum autobody panels, which provides a good correlation with lab testing and field performance.

### **Approach**

- Define test matrix.
- Specify and obtain materials.
- Specify phosphate and paint system.
- Pretreat and paint test specimens.
- Conduct laboratory corrosion testing.
- Perform outdoor exposure, test track, and in-service testing.
- Evaluate test data according to defined procedures.
- Revise second iteration of testing based upon initial data.

### **Accomplishments**

- Initiated laboratory, outdoor exposure, test track and in-service testing.
- Completed the first round of lab testing.

- Progressed with statistical analysis of the extent of corrosion on lab samples.
- Progressed with corrosion product analysis to support field—lab correlation.

**Future Direction**

- Complete analysis of lab test data from the first iteration
- Complete the corrosion product analysis study on lab test samples
- Progress toward second iteration of lab tests

**Background**

In the previous annual report, a description of the lab, test track, outdoor exposure, and in-service tests was provided as well as some general background on aluminum corrosion mechanisms. In this year’s report, the focus will be on data analysis from the first iteration of lab tests, which have been completed.

**Panel Evaluation**

**Goals of Analysis**

The evaluation of the corrosion test panels is critical for the Aluminum Automotive Closure Panel Corrosion Test Program. The goal is to correlate accelerated testing to in-service performance. However, the method used to date for evaluation has been a visual inspection that is highly operator, or

evaluator, dependent. The team has sought a more robust method for evaluation that is more quantitative. The Atlas View system has provided a good method for this evaluation that eliminates the variations from one operator to the next. It is hoped that this technique will eliminate much of the “art” associated with visual evaluation and provide more consistency to corrosion test results.

**Atlas View**

The View technique is a digital image analysis method that can measure the maximum creepback from the scribe, the average creepback about the scribe, and the area affected by corrosion around the scribe line. The system uses direct light to identify the areas affected by corrosion. Panels analyzed by the system must be flat to eliminate errors associated with shadows. Figure 1

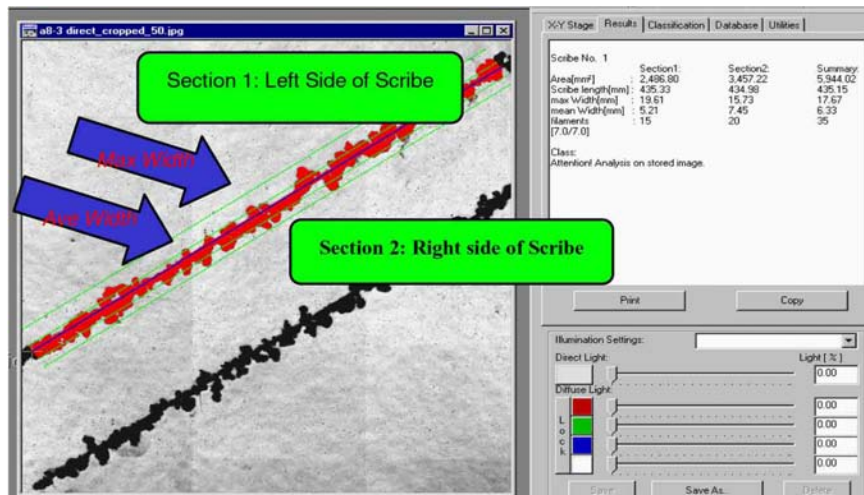


Figure 1. Typical output from the View system.

shows typical output from the View system. The Atlas terminology of width means the length of the creepback used in this paper.

One question posed by the team was whether the View method correlates with the industry-accepted method of visual evaluation. A subset of the team visually evaluated multiple panels; those results were then compared with the output of the View method. A sampling of the results is given in Figure 2.

These charts show the visual evaluations for maximum creepback of three different operators/evaluators compared with the maximum creepback identified using the View image analyzer. Multiple panels were evaluated visually, and the View output correlated well with all of the visual measurements.

The next question was to determine which outputs the team should use from the View. The outputs from the View include maximum creepback, average creepback from the scribe line, and area of corrosion about the scribe line. Figure 3 shows the correlation of the visual maximum creepback from the scribe to the Atlas average creepback for panels exposed to an accelerated corrosion test. The test was conducted at two laboratories and the results are compiled in Figure 3.

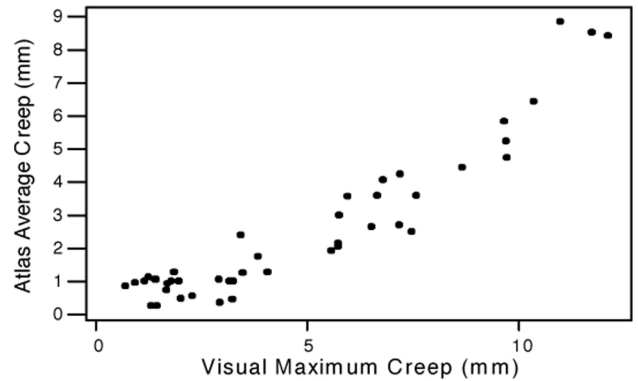


Figure 3. Results of lab tests.

The regression equation is

$$\text{Atlas average creep} = -0.556 + 0.639 \text{ visual max creep}$$

$$R\text{-Sq} = 86.7\% \quad R\text{-Sq(adjusted)} = 86.4\%$$

The results show good correlation between the Atlas average creepback and the visual maximum creepback, with an adjusted R-squared of 86%. The average creepback is difficult to measure in a visual evaluation, although it can be done. The average creepback provides clues on the extent of corrosion along the length of the scribe. Maximum creepback can be deceptive, because it may represent only a single filiform along the scribe, whereas average creepback

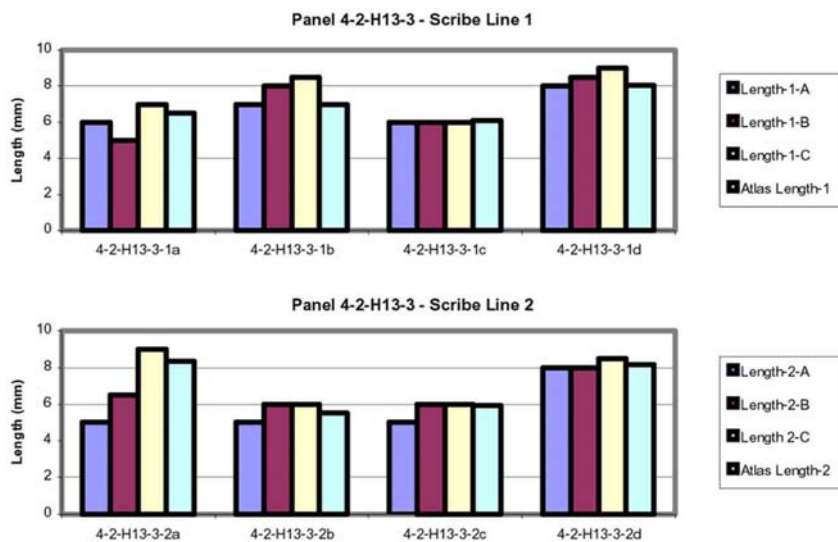


Figure 2. Visual evaluations for maximum creepback.

indicates the extent of corrosion along the entire length of the scribe.

A correlation was also established between Atlas maximum creepback and visual maximum creepback. The limitations of looking only at maximum creepback have been discussed, but once again there is good correlation between visual and Atlas data, as shown in Figure 4.

The regression equation is

$$\text{Atlas max} = 1.71 + 0.789 \text{ vis eval max}$$

$$R\text{-Sq} = 79.8\% \quad R\text{-Sq}(\text{adj}) = 79.3\%$$

Although the adjusted R-squared is not quite as good as when the visual maximum creepback was correlated to the Atlas average creepback, there is still a strong correlation between visual maximum creep and Atlas maximum creep.

A similar analysis was done to determine if Atlas area of corrosion correlates to visual maximum creepback. The results of the analysis are given in Figure 5.

The regression equation is

$$\text{Atlas area} = -83.8 + 106 \text{ visual max creepback}$$

$$R\text{-Sq} = 83.9\% \quad R\text{-Sq}(\text{adj}) = 83.6\%$$

The Atlas area of corrosion correlates to the visual maximum creepback in a very similar manner to the correlation of Atlas average creepback to visual maximum creepback.

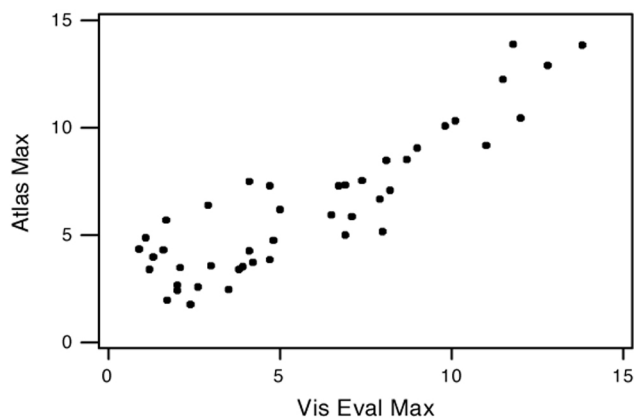


**Figure 4.** Correlation between visual and Atlas data.

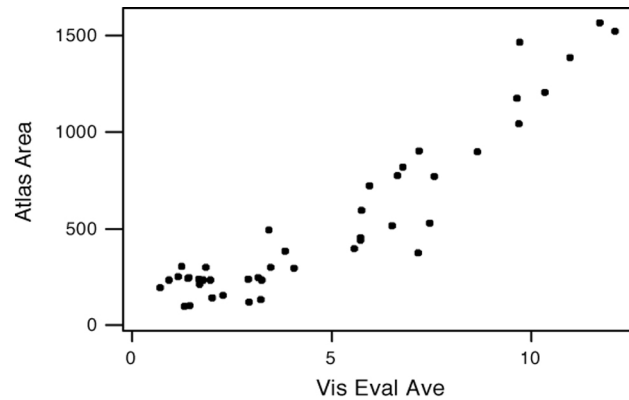


**Figure 5.** Results of the analysis.

Area of corrosion and average creepback are similar measures and could very likely be used interchangeably. For the data used to generate the above graphs, Atlas average creepback predicted Atlas area with an adjusted R-squared of 94%. It is expected that a similar correlation will be found for any data set of this type.

As a result of this study, the team gained confidence in using the Atlas View method to evaluate corrosion performance. Additional work is still necessary to determine which output (area, maximum creep, average creep) or combination of outputs is necessary to fully understand corrosion performance. It is likely that a sampling of panels exhibiting varying levels of corrosion performance will need to be visually ranked and the Atlas data then correlated to that ranking. This has not yet been done, but it will be included in the next phase of evaluation.

To date the first round of accelerated testing has been completed. All of the panels that have undergone accelerated testing have been scanned using the Atlas View and evaluated. The data are currently being analyzed by a statistician (Duncan McCune) to determine whether the panels show differences in corrosion performance. The statistician will also evaluate if the testing laboratory has an effect on corrosion performance when the same accelerated test is run.

The team also has test panels on the original equipment manufacturer (OEM) test tracks, in outdoor exposure, and on

in-service vehicles. Those panels will also be evaluated using the Atlas Vieew at the end of testing, as well as during regular intervals of testing whenever possible. A key evaluation criterion is to ensure that the mode of corrosion exhibited on in-service vehicles is the

same as that exhibited during accelerated corrosion testing. We hope to also get data to understand the method of initiation of corrosion to determine which testing best predicts in-service performance.

## **E. Development of the Infrared Thermal Forming Process for Production of Aluminum Vehicle Components**

*Principal Investigator: G. Mackiewicz-Ludtka*

*Oak Ridge National Laboratory*

*P.O. Box 2008, Oak Ridge, TN 37831-6080*

*(865) 576-4652; fax: (865) 574-4357; e-mail: ludtkagm@ornl.gov*

*Technology Area Development Manager: Joseph A. Carpenter*

*(202) 586-1022; fax: (202) 586-1600; e-mail: joseph.carpenter@ee.doe.gov*

*Field Technical Manager: Philip S. Sklad*

*(865) 574-5069; fax: (865) 576-4963; e-mail: sklads@ornl.gov*

---

*Contractor: Oak Ridge National Laboratory*

*Prime Contract No.: DE-AC05-00OR22725*

---

### **Objective**

- Implement infrared (IR) thermal forming as a preform method for aluminum tubes prior to hydroforming to reduce vehicle weight and achieve greater fuel economy.
- Verify initial IR thermal forming estimates to determine concept feasibility for aluminum tubes.
- Develop IR thermal forming process to form basic preform aluminum tubes for subsequent hydroforming trials.
- Evaluate IR thermally formed tubes after hydroforming.

### **Approach**

- Initiate a 1-year feasibility study, followed by longer-term activities (based on favorable results from this feasibility effort) to address the following four primary process concerns: (1) a process that produces bends in the tubes, (2) a process that can meet production rates required for automotive needs, (3) an estimated cost associated with the process and how it compares to present processes, and (4) the influence of the process on the applications, that is, effects on material properties.

### **Accomplishments**

- Verified initial IR thermal forming estimates to determine concept feasibility for aluminum tubes. Verified order-of-magnitude for thermal forming time estimates using the IR process. Forming of a 45° bend is estimated to be achieved in 5–20 s. Results suggest that a minimum of ~5 s is required using optimized processing with cooling, and a range of 10–20 s without cooling.
- Completed initial basic experiments on thin plates, demonstrating the need for a more fundamental approach to bend the significantly more complex tube geometry.
- Identified preliminary IR heat flux issues to be addressed to form basic preform aluminum tubes for subsequent hydroforming trials.

- Developed initial modeling methodology and initiated preliminary model simulations that successfully predict IR thermal processing trends.
- Completed experimental and simulation modeling trials that indicate that further optics development and validation phases will be necessary to achieve the power distribution required to conform larger tubes to the shape needed for hydroforming preforms.

### Future Direction

- Redesign and refine the IR thermal forming system as needed (reflector shape, focal length, power density, and cooling) for the more complex case of thermally forming tubes.
- Develop the appropriate reflector design (optics), based on initial experimental and simulation modeling results, that will enable the thermal flux contouring and the correct heat (power) distribution needed for preforming larger tubes to the shape needed for hydroforming preforms.
- Validate optics performance to achieve the power distribution required to form larger tubes to the shape needed for hydroforming preforms.
- Continue tube bending trials utilizing the newly designed IR thermal forming system to successfully bend a tube to be tested in hydroforming trials.

### Introduction

During the last 9 years, N. A. Technologies (NAT) initiated thermal forming research utilizing the *laser* as the heat source. Using the laser, NAT has formed a wide variety of tubes in various sizes and materials. The laser thermal forming process has been found to work on both large and small aluminum tubes (see Figure 1). These experiments have demonstrated that the wall thickness of the outside bend of the tube is virtually unaffected and the inside bend actually thickened in all cases. However, the cycle times required for laser forming are too long to be considered for high-volume applications. Based on some work done on plate-stock, NAT has shown that if the thermal input power level is scaled-up from 4 kW (characteristic of laser technology) to 300 kW (characteristic of IR plasma lamp), IR thermal forming works similarly, but much faster. However, this process still has to be proven for tubes. Consequently, the Vortek lamp that is installed at Oak Ridge National Laboratory (ORNL), with its inherent power levels, offers the potential to move the thermal forming process to speeds that are high enough to



**Figure 1.** Laser thermal forming process has been demonstrated on small aluminum tubes.

reach production rate levels. In fact, the higher power levels available with the Vortek lamp are key to taking this process from the “prototyping” or low-volume production stage, to the actual high-volume production stage. NAT has estimated that utilizing the power capacity of the Vortek lamp, the

thermal forming process can be put into *actual production (i.e., 60 units/h, as opposed to 2 units/h that can be achieved in the laser lab today)*. The key to tapping this higher power source to thermally form the tubes will be developing the correct heat distribution profile.

To date, a great deal of effort has been spent on finite-element modeling at Massachusetts Institute of Technology (MIT), Boeing, Rockwell, Penn-State, Ohio State, British Aerospace, and the best results (from MIT) provide predictions that are off by  $\pm 50\%$ . These results emphasize the complexity of the IR thermal forming process. This complexity results directly from the extreme, transient nature of the process with continuously varying surface boundary conditions. Consequently, considerable work remains to be done to develop this process to distribute the heat properly around the tube. NAT has spent nearly a decade developing an understanding of the heat distribution needed to laser form a tube. Developing this process to distribute the heat from the Vortek heat source properly around the tube will be a significant effort. NAT is optimistic that, based on its success at scale-up of plate using the neural-network-based model,\* developing the right thermal distribution with the Vortek lamp is possible. Success will be defined as demonstrating that the IR thermal forming process works and that it has the possibility of scale-up to real production.

Building on the NAT experience with laser forming and the results from the preliminary experiments involving the IR thermal forming process completed as part of the MPLUS program at ORNL, this project holds the promise of achieving DOE goals of reducing vehicle weight to realize greater fuel economy. The high thermal heat source of the IR lamp technology holds the key to unlock the potential in demonstrating that

the IR thermal forming process is more than a laboratory demonstration so that the energy savings potential can be realized.

## **Status and Annual Summary—Feasibility Study**

### **Introduction and Background**

From the onset of this project, as noted above, it has been known that developing the thermal forming process to properly distribute the heat flux around the tube would be a significant effort. However, based on NAT successful results using laser forming on small-diameter tubes, and its subsequent success at trial scale-up efforts for translating these results to plate, with the neural-network-based model developing the right thermal distribution with the Vortek lamp seems very viable. Consequently, a preliminary *feasibility study* was initiated. Due to the limited project budget available in the first year, the most cost-effective approaches were attempted first to verify the viability of utilizing IR thermal forming to form tubes. Several experimental approaches were attempted to determine the concept feasibility of utilizing IR thermal forming as a fixtureless preforming operation for subsequently hydroformed aluminum vehicle components. These approaches were (1) adapting a long (4-cm) stand-off reflector that was available, (2) modifying the hardware below the reflector to obtain a smaller thermally controlled heat flux zone (thermal footprint), and (3) developing and testing a thermal processing model to run process simulations to determine the appropriate reflector design needed to produce the correct heat flux distribution around the tube. These cost-efficient methods/steps are described below.

### **Hardware Modifications**

In the first attempt, the optics selected and utilized were those that enabled the largest (4-cm) stand-off from the work piece. To accomplish this, the already available

---

\*Trained neural networks are attractive predictors for manufacturing processes because they can accurately capture material/process response without requiring actual physical data/models.

4-cm IR reflector optics were redesigned/reworked to attempt to provide the thermal flux and thermal footprint necessary to thermally bend tubes. Results from these experiments determined that a narrower beam and a higher heat flux are needed. To address this issue, a water-cooled, focusing plate was designed and fabricated to assist in controlling this heat input. The motive behind this inexpensive attempt was to constrain the heat flux at the surface of the tube by merely blocking and absorbing the heat outside of the targeted thermal footprint zone of the IR beam. Experimental trials, however, determined that not enough heat was available to form tubes because the thermal contour was not optimized yet for the tube geometry. However, these experiments did confirm the need to gain a more fundamental understanding of the heat flux required to design an IR thermal forming system in order to address the more complex case of thermally forming tubes. To accomplish this goal, an IR thermal forming system is needed to address several issues, including reflector shape, focal length, power density, and cooling.

### Basic Experimental Trials

Initial IR thermal forming trials on 4-in.-diam tubes demonstrated the need for a more fundamental understanding of the thermal flux and approach needed to bend the significantly more complex tube geometry. To gain this fundamental understanding of the IR thermal forming process, basic experimental studies were initiated on thin plates instrumented with thermocouples (Figure 2). The purpose of these trials was first to obtain experimental temperature data to guide the selection of the heat flux needed to form aluminum plates and later extend this methodology to the more complex case of forming the tube geometry.

An example of the experimental setup used during the basic study trials is

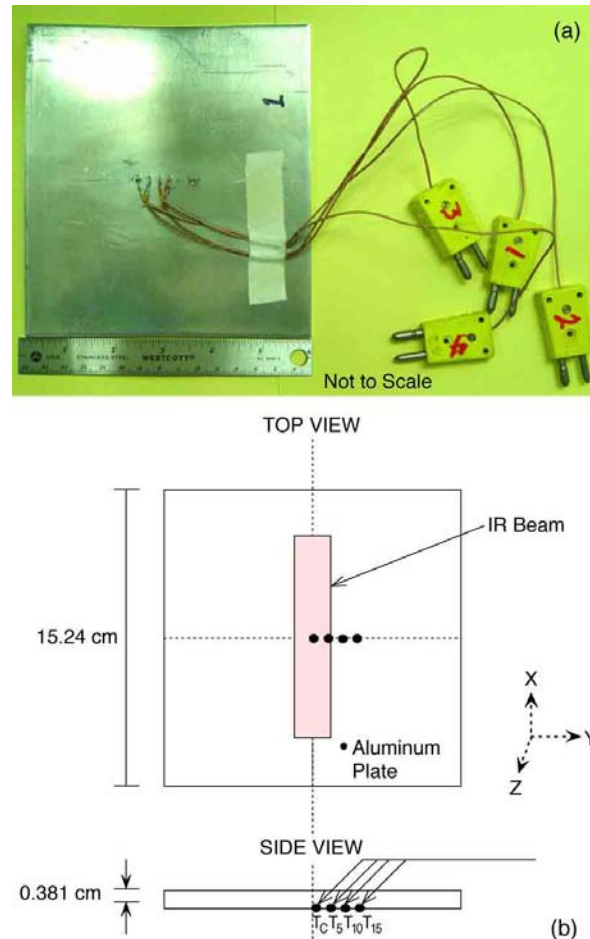


**Figure 2.** Experimental thermal forming specimens were instrumented during trials to gain a more fundamental understanding of the IR thermal forming process.

demonstrated in Figure 3(a). Figure 3(b) exhibits an example of the plate deflection obtained for a 0.125-in.-thick aluminum plate based on initial study.

To gain a more basic understanding of how the heat flux distribution needs to be tailored to obtain the amount of tube bending necessary to bend tubes, these initial experimental processing trials used a stationary IR pulse, and the resultant temperature was measured as a function of time at increasing distances from the heat source. The temperature was measured by thermocouples attached to the aluminum on the side opposite the IR source (Figure 2).

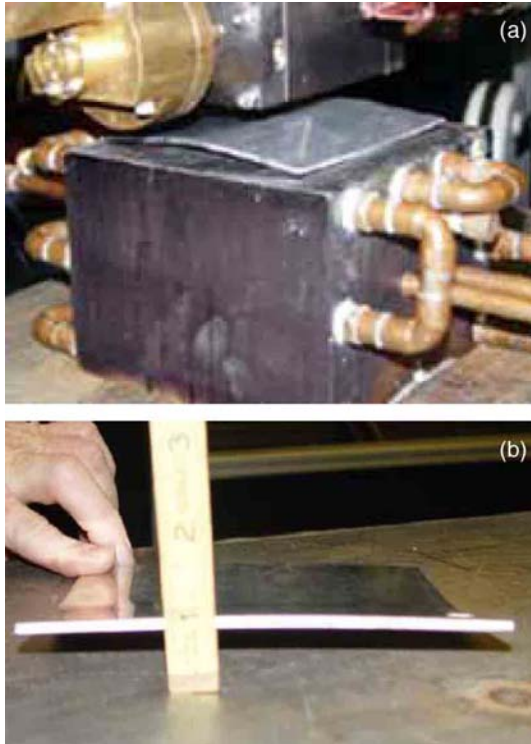


**Figure 3.** Examples of (a) the IR thermal forming setup and (b) the aluminum plate deflection observed during initial experimental IR thermal forming trials.

### Thermal Forming Simulations

To gain a more fundamental insight into the heat flux power distribution required to

conform larger tubes to the shape needed for hydroforming preforms and to guide us in the redesign of the IR forming system, a preliminary modeling methodology was developed first for the case of a flat plate. The modeling cases were set up to simulate the thermal processing conditions utilized during the basic experimental trials. Therefore, modeling simulations were run using the experimental parameters as a guide in setting up the modeling boundary conditions. Thermophysical parameters used for the simulations were obtained from the literature. The resulting model predictions were evaluated and compared with the experimental results. These preliminary model simulations successfully predicted the temperature trends observed during the experimental IR processing trials (Figure 4). To better understand and predict the influence of heat flux on the amount of deflection, a finite-element model also was set up and used to analyze the stresses resulting from the thermal processing parameters. The mechanical response of the aluminum plate to thermal forming process parameters was evaluated. Model assumptions for this analysis were as follows:

- Faces on  $x = 0$  and  $y = 0$  were constrained to be symmetry planes.

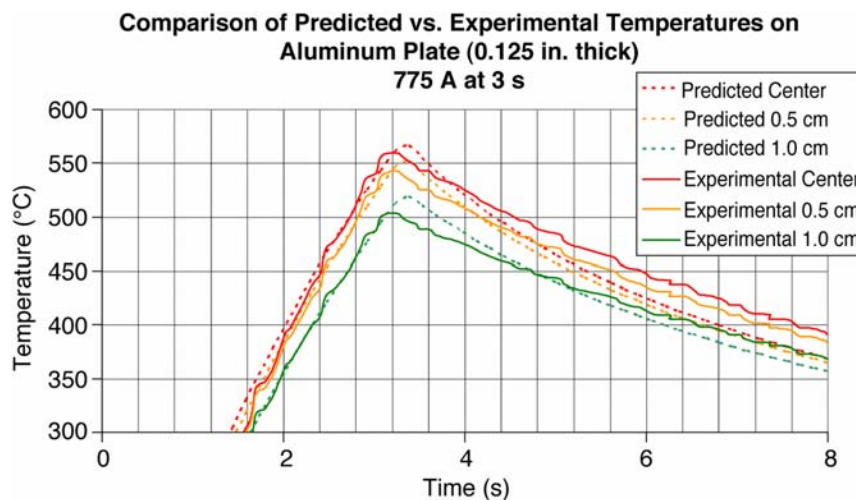


**Figure 4.** Comparisons between experimental results and modeling simulation predictions demonstrate excellent agreement.

- Bottom edge along  $x = x_{max}$  was constrained to have zero displacement along x-direction.
- Bottom edge along  $y = y_{max}$  was constrained to have zero displacement along y-direction.
- Bottom node at  $x = 0$  and  $y = y_{max}$  was fixed to have no vertical displacement.

The modeling results successfully predict the same degree of plate deflection as those measured/obtained from the initial basic experimental study trials (see Figure 5).

A parametric study also was done (using these initial nonoptimized experimental

results) as a method of estimating deflections anticipated based on plate thickness and the maximum heat flux input into the aluminum plates. These results (Table 1) indicate that as the maximum heat flux is increased, the deflection increases, and that as the plate thickness decreases, the plate deflects significantly more. Of course, the thicker plate also cools much more slowly, and additional localized cooling, applied immediately after heating likely would provide the necessary constraint to enhance bending. This would also be true for the thinner plate.

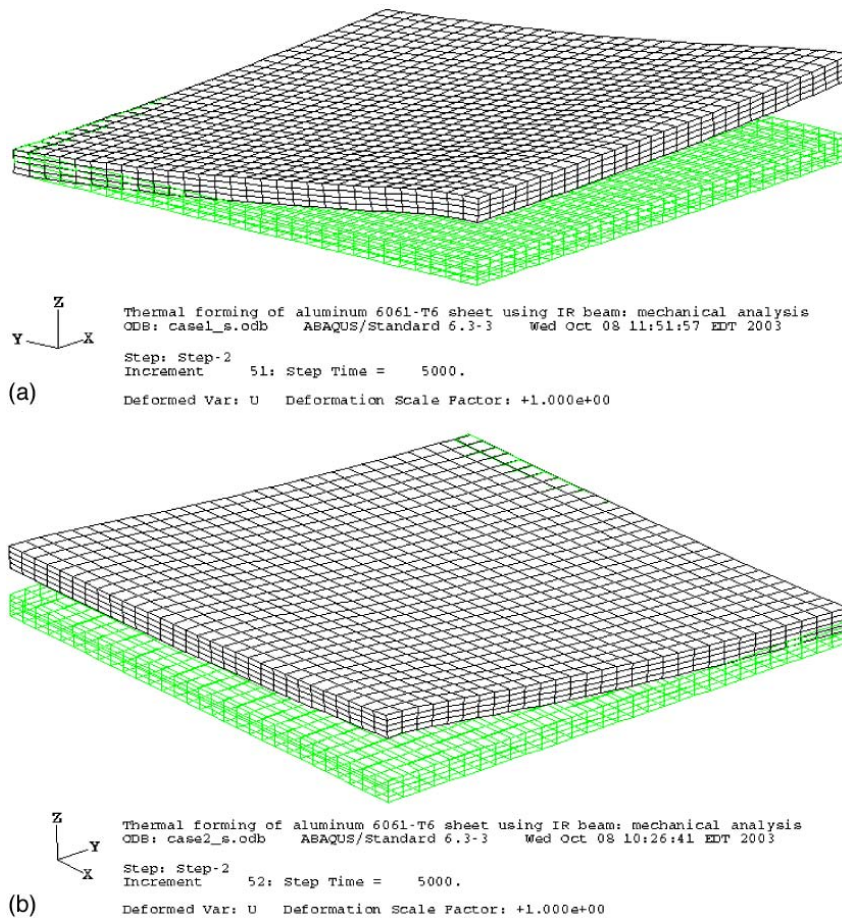


**Figure 5.** Modeling results demonstrating excellent agreement with finite-element stress analysis predictions for 0.125-in.-thick plate at the end of cooling step for two heat fluxes: (a) the deflection along the plate center relative to the edge, and (b) the small deflection of the corner opposite to the origin.

**Table 1.** Parametric modeling study results

Plate thickness (in.)	Maximum heat flux (W/mm <sup>2</sup> )	Maximum temperature (°C)	Maximum deflection (mm)
0.125	2.25	641	10.92
0.125	2.0	574	9.58
1.0	2.25	203	0.016
1.0	2.0	184	0.014

Both experimental and simulation modeling results indicate that further optics development and validation phases will be necessary to achieve the power distribution required to conform larger tubes to the shape needed for hydroforming preforms.

**Neural Net Modeling Results**

To gain some insight into what the optimized thermal processing parameters need to be to thermally form an aluminum plate, a neural net model has been developed based on the initial experimental trials.

Results for the experimentally designed matrix determined that the maximum deflection can occur within the following processing parameter windows:

- Example 1
  - Lamp power: 755 A
  - Pulse duration: 3 s
  - Defocus: 16 mm
- Example 2
  - Lamp power: 815 A
  - Pulse duration: 3.3 s
  - Defocus: 20.8 mm

The model allows one to vary each of the three processing parameters independently, and/or as a group to assist in determining the most suitable set of processing parameters defined within the experimental data limits. Figure 6 depicts the graphical 3-D space within which one can determine the processing parameters to obtain the maximum deflection using the neural net modeling approach to graph a composite plot from which to estimate either the deflection per IR pulse, the number of pulses to obtain a 45° deflection angle, or the total time

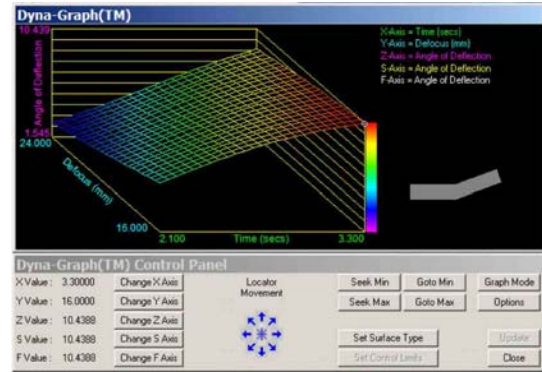


**Figure 6.** Graphical 3-D representation of neural net modeling results, indicating maximum deflection based on initial experimental trials.

necessary to obtain a 45° bend within the experimentally designed limits (see Figure 7). Our best results to date estimate excellent cycle times to thermally bend a tube to a 45° angle, even based on these nonoptimized, in-progress IR results. Model-predicted cycle time estimates are as follows:

1. a minimum of ~5 s using optimized processing with cooling;
2. a range of 10–20 s without cooling;
3. a maximum of 98 s for this nonoptimized data set.

Additional experiments are in progress to further optimize cycle times within broader processing limits. The next step will be to apply the knowledge gained from these plate

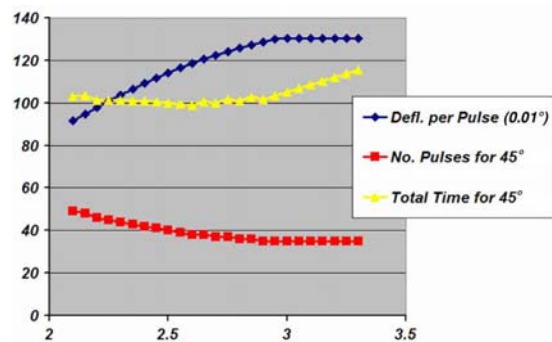


**Figure 7.** Neural network modeling results depicting the initial response diagram, indicating the sets of processing parameters that produce the maximum plate deflection, based on initial set of basic experimental trials.

results to develop the thermal forming processing parameters to form a tube.

### **Thermal Forming Current Status**

Within the feasibility phase of this project, initial IR trials based on flat plates for thermal forming aluminum tubes have verified the relative order-of-magnitude of time estimates using the IR process. Forming of a 45° bend is estimated to be achieved in 5–20 s. Results suggest that a minimum of ~5 s is required, using optimized processing with cooling and a range of 10–20 s without cooling.

Currently, as part of the concept feasibility demonstration, work is under way to redesign and refine the IR thermal forming system as needed (reflector shape, focal length, power density, and cooling) for the more complex case of thermally forming tubes. This effort will include developing the appropriate reflector design (optics), based on initial experimental and simulation modeling results, that will enable the thermal flux contouring and the correct heat (power) distribution needed for preforming larger tubes to the shape needed for hydroforming preforms. Following this, optics performance to achieve the power distribution required for forming larger tubes to the shape needed for hydroforming preforms will be validated, and tube bending trials will continue utilizing the newly designed IR thermal forming system to successfully bend a tube to be tested in hydroforming trials.

### **Future Work**

Current plans for Phase 3 tasks are as follows: (1) Bend full-size tubes. (2) Characterize and compare IR vs

conventionally formed microstructures and properties for bent tubes. (3) Provide bent tubes to industry for hydroforming trials. (4) Evaluate material response, microstructure, and properties of posthydroformed IR processed tubes. (5) Optimize the IR thermal forming process to achieve bend required for subsequent hydroforming. (6) Utilize modeling to guide the thermal forming process development and optimization.

### **Conclusions**

- Within the feasibility phase of this project, initial IR trials based on flat plates for thermal forming aluminum tubes have verified the relative order-of-magnitude of time estimates using the IR process. Forming of a 45° bend is estimated to be achieved in 5–20 s. Results suggest that a minimum of ~5 s is required using optimized processing with cooling, a range of 10–20 s without cooling.
- Both experimental and simulation modeling results indicate that further optics development and validation phases, in addition to cooling control, will be necessary to achieve the power distribution required to conform larger tubes to the shape needed for hydroforming preforms.
- We have completed initial experiments on thin plates to obtain the information; we need to redesign the system (reflector shape, focal length, power density, and cooling) for the more complex case of thermally forming tubes.
- The appropriate reflector design will be developed to provide the thermal flux contouring needed for forming tubes.